

PB90-162330

**BEDROCK ACCELERATIONS IN MEMPHIS AREA  
DUE TO LARGE NEW MADRID EARTHQUAKES**

by

H.H.M. Hwang<sup>1</sup>, C.H.S. Chen<sup>2</sup> and G. Yu<sup>3</sup>

November 7, 1989

Technical Report NCEER-89-0029

NCEER Contract Number 88-3016

NSF Master Contract Number ECE 86-07591

- 1 Associate Research Professor, Center for Earthquake Research and Information, Memphis State University
- 2 Research Associate, Center for Earthquake Research and Information, Memphis State University
- 3 Graduate Research Assistant, Center for Earthquake Research and Information, Memphis State University

NATIONAL CENTER FOR EARTHQUAKE ENGINEERING RESEARCH  
State University of New York at Buffalo  
Red Jacket Quadrangle, Buffalo, NY 14261

---

REPRODUCED BY  
U.S. DEPARTMENT OF COMMERCE  
NATIONAL TECHNICAL  
INFORMATION SERVICE  
SPRINGFIELD, VA 22161



REPORT DOCUMENTATION PAGE	1. REPORT NO. NCEER-89-0029	2.	3. Recipient's Accession No.
4. Title and Subtitle Bedrock Accelerations in Memphis Area Due to Large New Madrid Earthquakes		5. Report Date November 7, 1989	
7. Author(s) H.H.M. Hwang, C.H.S. Chen and G. Yu		6.	
9. Performing Organization Name and Address		8. Performing Organization Rept. No.	
		10. Project/Task/Work Unit No.	
		11. Contract(C) or Grant(G) No. (C) 88-3016 and (G) ECE 86-07591	
12. Sponsoring Organization Name and Address National Center for Earthquake Engineering Research State University of New York at Buffalo Red Jacket Quadrangle Buffalo, New York 14261		13. Type of Report & Period Covered Technical Report	
15. Supplementary Notes This research was conducted at Memphis State University and was partially supported by the National Science Foundation under Grant No. ECE 86-07591.		14.	
16. Abstract (Limit: 200 words)  Memphis and Shelby County are geographically close to the southern segment of the New Madrid seismic zone (NMSZ). The NMSZ is being regarded by seismologists and earthquake engineers as the most hazardous zone in the eastern United States. In this study, a seismologically-based model is utilized to describe the horizontal bedrock motions at a site due to primarily shear waves generated from a seismic source. This model is centered on a power spectrum which is in turn developed from a seismologically-based Fourier amplitude spectrum. From the power spectrum, earthquake time histories and probability-based response spectra can be generated directly. The power spectrum generated in this study can also be used to estimate the peak value of earthquake acceleration based on the extreme value distribution of a random process. The peak values of horizontal bedrock accelerations for Memphis and Shelby County are computed for two New Madrid earthquakes of $M = 7.5$ and $6.5$ . Two different cases of seismic sources are considered: (1) a single source at Marked Tree, Arkansas, and (2) the southern segment of the NMSZ. The results are presented in contour maps.			
17. Document Analysis a. Descriptors			
b. Identifiers/Open-Ended Terms EARTHQUAKE ENGINEERING                      LIFELINE SYSTEMS                      MEMPHIS, TENNESSEE INFRASTRUCTURES                              BEDROCK MOTIONS                      BEDROCK ACCELERATION SHELBY COUNTY, TENNESSEE                      SEISMOLOGY SEISMIC RISK ASSESSMENT NEW MADRID SEISMIC ZONE (NMSZ) c. COSATI Field/Group			
8. Availability Statement Release Unlimited		19. Security Class (This Report) Unclassified	21. No. of Pages
		20. Security Class (This Page) Unclassified	22. Price



## PREFACE

The National Center for Earthquake Engineering Research (NCEER) is devoted to the expansion and dissemination of knowledge about earthquakes, the improvement of earthquake-resistant design, and the implementation of seismic hazard mitigation procedures to minimize loss of lives and property. The emphasis is on structures and lifelines that are found in zones of moderate to high seismicity throughout the United States.

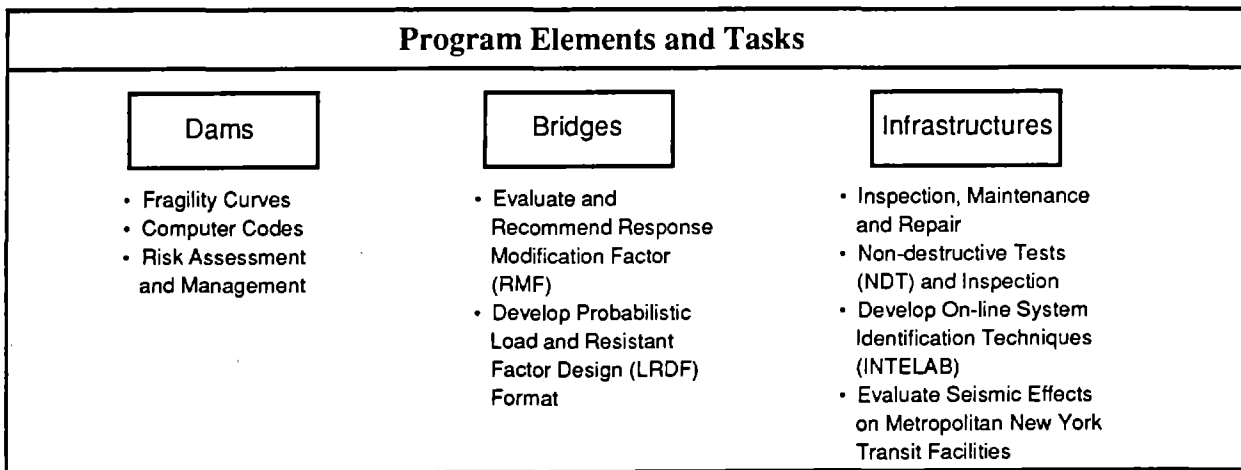
NCEER's research is being carried out in an integrated and coordinated manner following a structured program. The current research program comprises four main areas:

- Existing and New Structures
- Secondary and Protective Systems
- Lifeline Systems
- Disaster Research and Planning

This technical report pertains to Program 3, Lifeline Systems, and more specifically to the study of dams, bridges and infrastructures.

The safe and serviceable operation of lifeline systems such as gas, electricity, oil, water, communication and transportation networks, immediately after a severe earthquake, is of crucial importance to the welfare of the general public, and to the mitigation of seismic hazards upon society at large. The long-term goals of the lifeline study are to evaluate the seismic performance of lifeline systems in general, and to recommend measures for mitigating the societal risk arising from their failures.

In addition to the study of specific lifeline systems, such as water delivery and crude oil transmission systems, effort is directed toward the study of the behavior of dams, bridges and infrastructures under seismic conditions. Seismological and geotechnical issues, such as variation in seismic intensity from attenuation effects, faulting, liquefaction and spatial variability of soil properties are topics under investigation. These topics are shown in the figure below.



*In this study, a seismologically-based stochastic model is utilized to describe the horizontal bedrock motions at a site in Shelby County, Tennessee due primarily to shear waves generated from the New Madrid seismic source. This stochastic model is based on a power spectrum which in turn is developed from a seismologically-based Fourier amplitude spectrum. From the power spectrum, earthquake time histories and probability-based response spectra can be generated directly. The peak values of horizontal bedrock accelerations for Memphis and Shelby County are computed for two New Madrid earthquakes of  $M = 7.5$  and  $6.5$ . Two different cases of seismic sources are considered: (1) a single source at Marked Tree, Arkansas and (2) the southern section of the New Madrid seismic zone. The results are presented in contour maps.*

## ABSTRACT

↓  
Memphis and Shelby County are geographically close to the southern segment of the New Madrid seismic zone (NMSZ). The NMSZ is being regarded by seismologists and earthquake engineers as the most hazardous zone in the eastern United States. In this study, a seismologically-based model is <sup>used</sup> utilized to describe the horizontal bedrock motions at a site due to primarily shear waves generated from a seismic source. This model is centered on a power spectrum which is in turn developed from a seismologically-based Fourier amplitude spectrum. From the power spectrum, earthquake time histories and probability-based response spectra can be generated directly. The power spectrum generated in this study can also be used to estimate the peak value of earthquake acceleration based on the extreme value distribution of a random process. The peak values of horizontal bedrock accelerations for Memphis and Shelby County are computed for two New Madrid earthquakes of  $M = 7.5$  and  $6.5$ . Two different cases of seismic sources are considered: (1) a single source at Marked Tree, Arkansas; and (2) the southern segment of the NMSZ. The results are presented in contour maps. ↗





## TABLE OF CONTENTS

SECTION	TITLE	PAGE
1	INTRODUCTION	1-1
2	NEW MADRID SEISMIC ZONE	2-1
2.1	Tectonic Setting	2-1
2.2	Seismic Source Zone	2-1
2.3	Attenuation	2-4
2.4	Occurrence Rate	2-6
3	BEDROCK MOTION MODEL	3-1
3.1	Fourier Amplitude Spectrum	3-1
3.1.1	Source Spectral Function	3-1
3.1.2	Scaling Factor	3-3
3.1.3	Diminution Function	3-4
3.1.4	Shape Filter	3-4
3.2	Power Spectral Density Function	3-7
3.3	Time Histories	3-7
3.4	Probability-Based Response Spectra	3-9
3.5	Comments on Parameter Uncertainties	3-13
4	PEAK BEDROCK ACCELERATIONS IN MEMPHIS AREA	4-1
4.1	Estimation of Peak Bedrock Accelerations	4-1
4.2	A Marked Tree Event	4-1
4.3	Southern Segment of NMSZ	4-4
5	CONCLUSIONS	5-1
6	REFERENCES	6-1
APPENDIX		
A	EXTREME VALUE DISTRIBUTION OF A RANDOM PROCESS	A-1



## LIST OF ILLUSTRATIONS

FIGURE	TITLE	PAGE
1-1	Epicenters of New Madrid Earthquakes	1-2
2-1	Block Diagram of Buried Reelfoot Rift Complex	2-2
2-2	New Madrid Seismic Zone	2-3
2-3	Isoseismal Map of the 1811 New Madrid Earthquake	2-5
2-4	Frequency-Magnitude Curve for New Madrid Earthquakes	2-7
3-1	Fourier Amplitude Spectrum (M = 7.5 and R = 50 km)	3-6
3-2	Power Spectrum (M = 7.5 and R = 50 km)	3-8
3-3	Example of Envelope Function and Earthquake Time History	3-10
3-4	Mean Bedrock Response Spectra of Various Moment Magnitudes	3-12
4-1	Grid Points in Shelby County	4-2
4-2	Boundary of the Southern New Madrid Seismic Zone	4-3
4-3	Contour Map of Mean Peak Accelerations (M = 7.5, Marked Tree Event)	4-6
4-4	Contour Map of Mean Peak Accelerations (M = 6.5, Marked Tree Event)	4-7
4-5	Contour Map of Mean Peak Accelerations (M = 7.5, Southern NMSZ)	4-9
4-6	Contour Map of Mean + S.D. Accelerations (M = 7.5, Southern NMSZ)	4-10
4-7	Contour Map of Maximum Accelerations (M = 7.5, Southern NMSZ)	4-11
4-8	Contour Map of Mean Peak Accelerations (M = 6.5, Southern NMSZ)	4-12
4-9	Contour Map of Mean + S.D. Accelerations (M = 6.5, Southern NMSZ)	4-13
4-10	Contour Map of Maximum Accelerations (M = 6.5, Southern NMSZ)	4-14



## LIST OF TABLES

TABLE	TITLE	PAGE
3-I	Summary of Parameters	3-5
4-I	Marked Tree Event	4-5
4-II	Distribution of Peak Values (Southern NMSZ, $M = 7.5$ )	4-8



## SECTION 1

### INTRODUCTION

City of Memphis and Shelby County, Tennessee are geographically close to the southern segment of the New Madrid seismic zone (NMSZ) (figure 1-1). The NMSZ is regarded by seismologists and engineers as the most hazardous seismic zone in the eastern United States. In the winter of 1811-1812, this zone produced three of the largest earthquakes known to have occurred in North America and hundreds of damaging aftershocks. At present, this zone is still quite seismically active. Thus, a significant potential of seismic hazard exists in Memphis and Shelby County.

Estimating the characteristics of bedrock motions due to large New Madrid earthquakes is an essential task for earthquake-resistant design of structures and seismic risk assessment studies such as the Seismic Risk Assessment of Memphis Water Delivery System project. For engineering applications, quantitative measures of earthquake shaking rather than qualitative description such as Modified Mercalli Intensity are required. Making these quantitative estimates is quite challenging due to the lack of strong motion data in the New Madrid region. In this study, a seismologically-based model for the horizontal bedrock accelerations is first established. Using this model, the power spectrum, time histories and response spectra at a site can be developed. In addition, the peak value of horizontal bedrock accelerations can be estimated based on the extreme value distribution of a random process. Peak bedrock accelerations resulting from two large New Madrid earthquakes of moment magnitudes 7.5 and 6.5 are estimated and displayed in contour maps for Memphis and Shelby County.

# New Madrid Seismic Zone : 1974 - 1988

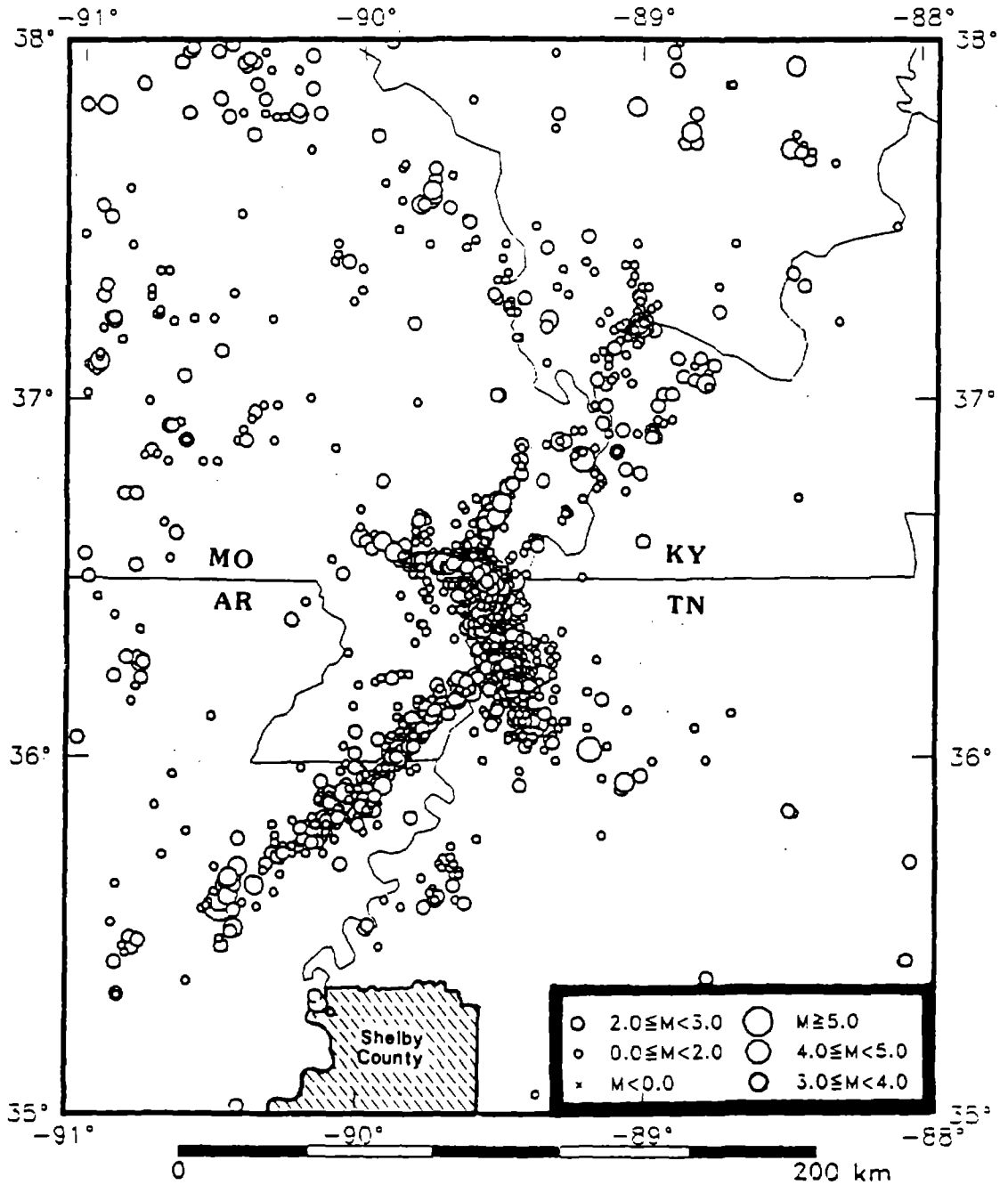


Figure 1-1 Epicenters of New Madrid Earthquakes



## SECTION 2

### NEW MADRID SEISMIC ZONE

#### 2.1 Tectonic Setting

The occurrence of large earthquakes in the middle of a continent is not well understood by seismologists and earthquake engineers. There is still no explanation of mid-plate earthquakes in plate-tectonic theory. However, it is now commonly believed that the present seismic activity in the New Madrid seismic zone (NMSZ) is related to an ancient rift complex known as the Reelfoot Rift Complex (figure 2-1) [1-7]. This continental rift of Late Precambrian age is expressed as a northeast trending graben in the granitic upper crust, filled with low-velocity sedimentary rocks. The rift is about 70 km wide and 200 km long. Both regional gravity and aeromagnetic surveys [7-9] and seismic refraction studies [10,11] support the rift complex hypothesis. Due to the present horizontal east-west compressive stress regime, the reactivation of the ancient faults within the rift complex is responsible for the earthquakes occurring in the NMSZ [4,12].

#### 2.2 Seismic Source Zone

At present, the NMSZ is still seismically active. Small earthquakes are detected almost every other day. The seismic zone is clearly delineated by the concentration of epicenters located by both the Memphis State University and Saint Louis University seismic networks (figure 2-2). From the pattern of epicenters, at least three distinct linear trends suggesting the orientations of three subsurface fault segments in the New Madrid region are observed [6,13,14]. These three fault segments are described as : (1) a southern segment extending from Marked Tree, Arkansas to Caruthersville, Missouri, roughly along the axis of the rift structure; (2) a middle segment trending northwest and extending from Ridgely, Tennessee to west of New Madrid, Missouri; and (3) a relatively shorter northern segment extending from west of New Madrid, Missouri to southern Illinois.

From the focal mechanism studies [6,12,15], both the northern and southern segments exhibit a predominately right-lateral strike slip fault-plane motion. The middle segment, on the other hand, appears to be more complex and exhibits a thrust faulting mechanism. According to Johnston [13], although the middle fault segment generates four times as

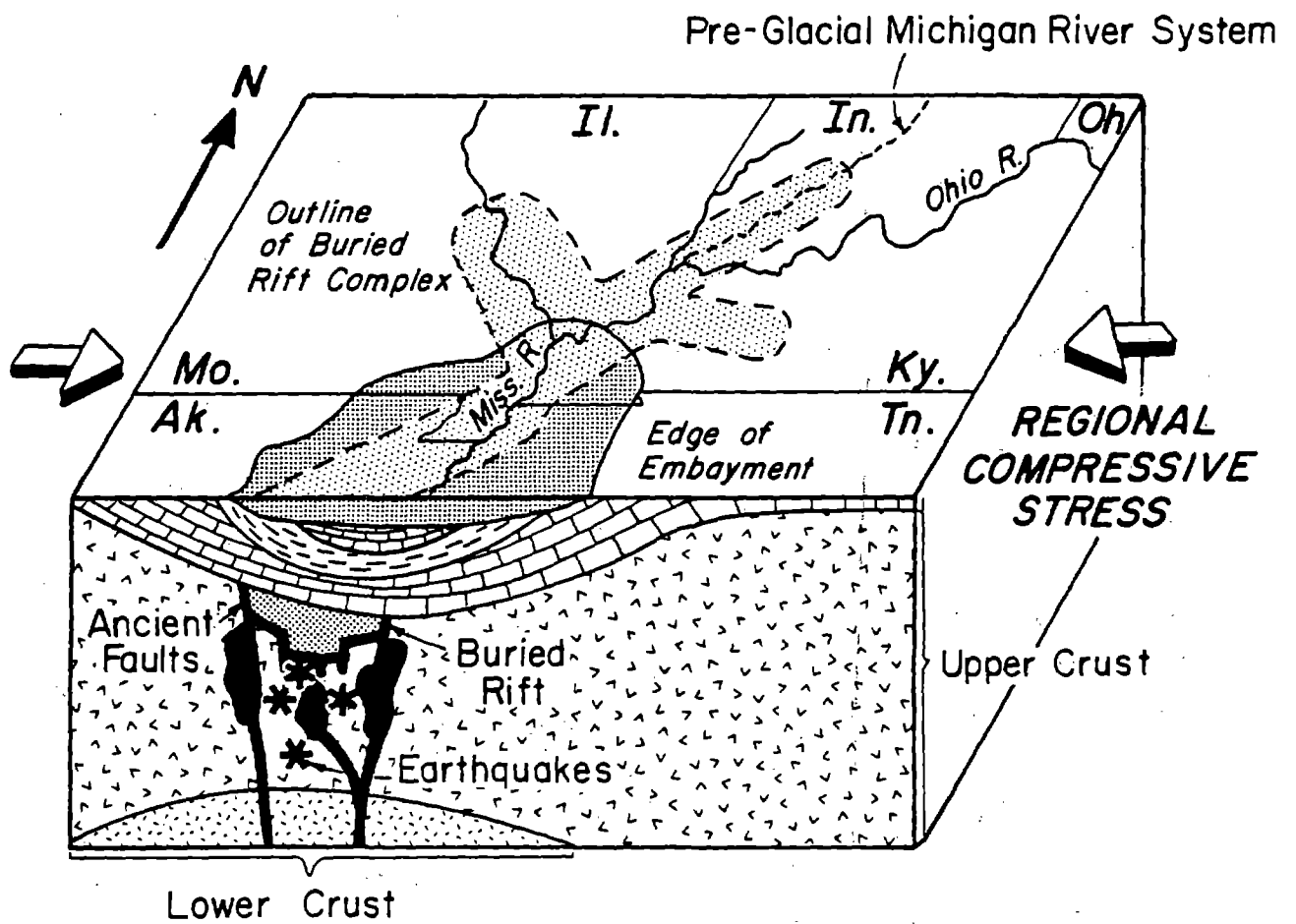


Figure 2-1 Block Diagram of Buried Reelfoot Rift Complex  
 (after Braile et al., 1982)

# New Madrid Seismic Zone : 1974 - 1988

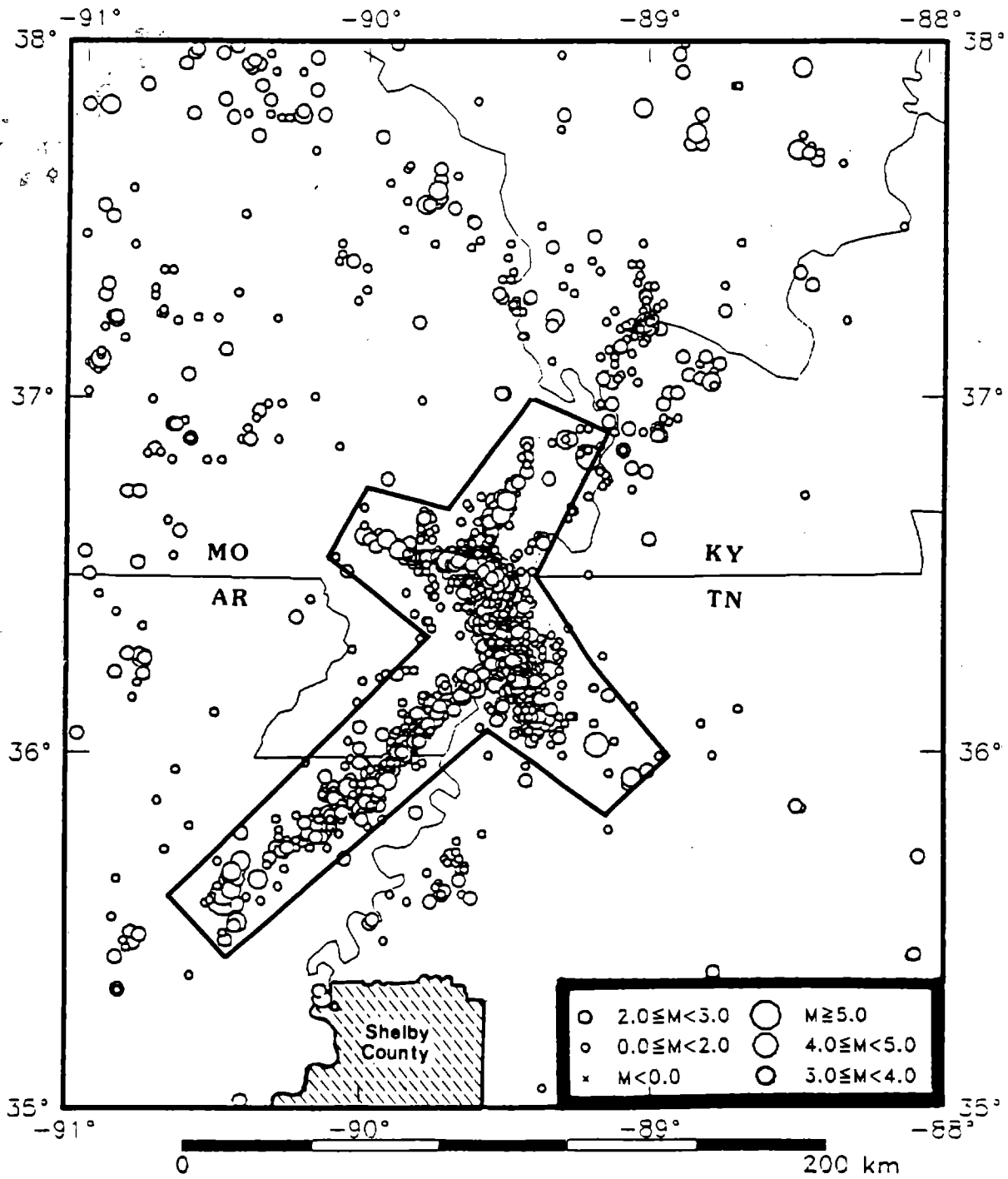


Figure 2-2 New Madrid Seismic Zone

many microearthquakes as the southern segment, it releases only one quarter of the seismic energy produced by the southern segment. Johnston further indicates that except along the three principal fault zones no earthquake of  $m_b \geq 6.0$  has occurred in the central United States. Thus, the NMSZ defined by Johnston [16] as shown in figure 2-2 is used in this study.

### 2.3 Attenuation

The 1811-1812 sequence of New Madrid earthquakes, according to Nuttli [17,18], produced damaging intensity at far greater than any other historical earthquake in North American continent. The shocks were felt over a wide area of central and eastern United States. Nuttli constructed a generalized isoseismal map of the first principal shock ( $M_s = 8.5$ ) occurred on December 16, 1811 (figure 2-3). The area experienced damaging earthquake motions (Modified Mercalli Intensity  $\geq$  VII) is estimated to be 600,000 km<sup>2</sup>.

The great distance at which the New Madrid earthquakes were felt and caused damages has been explained by low attenuation of the seismic waves in the central and eastern United States [18]. The attenuation of seismic waves is expressed by the quality factor  $Q$  which is dependent on frequency  $f$ . Based on the attenuation study conducted by Dwyer and others [19] in the central United States, the frequency dependent quality factor  $Q(f)$  of shear and  $L_g$  waves is

$$Q(f) = 1500 \cdot f^{0.4} \quad (2.1)$$

Several other  $Q$  models based on regional seismographic data have also been derived for the eastern North America (ENA). Hasegawa [20] analyzed the records of  $L_g$  waves from several Canadian shield events and proposed a  $Q$  factor for the Shields region as

$$Q(f) = 900 \cdot f^{0.2} \quad (2.2)$$

Shin and Herrmann [21] performed spectral analysis of the digitally recorded  $L_g$  waves of the New Brunswick aftershocks and suggested a  $Q(f)$  model as

$$Q(f) = 500 \cdot f^{0.65} \quad (2.3)$$

Since this study is related to NMSZ, we feel that the quality factor proposed by Dwyer and others [19] is more appropriate. Thus,  $Q(f)$  as shown in equation (2.1) is used.

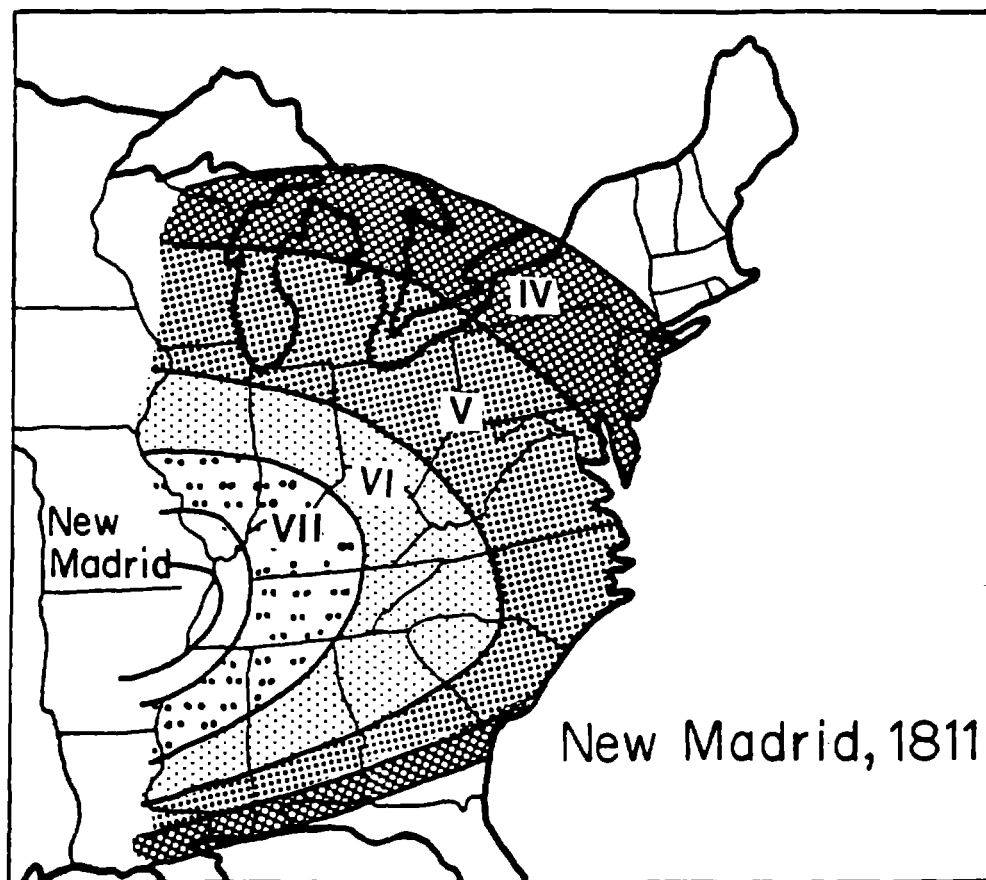


**Figure 2-3** Isoseismal Map of the 1811 New Madrid Earthquake  
(after Nuttli, O. W., 1973)

## 2.4 Occurrence Rate

Although a large New Madrid earthquake is known to have a much larger damaging area than that of a San Andreas earthquake of similar size [18], it is important to recognize that earthquakes occur more frequently in California than in the New Madrid region. A cumulative frequency-magnitude curve for the New Madrid earthquakes has recently been constructed by Johnston [16] as shown in figure 2-4.

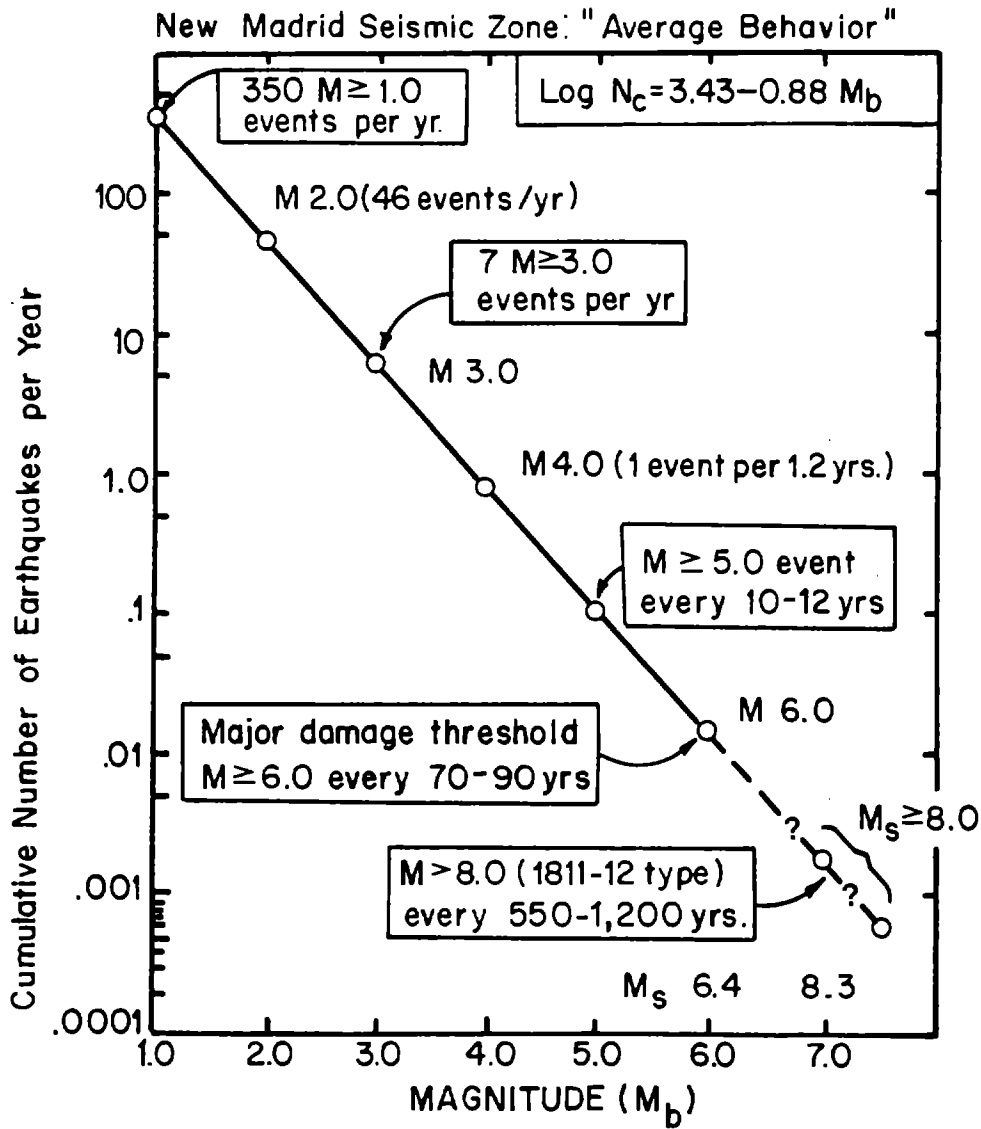


**Figure 2-4** Frequency-Magnitude Curve for New Madrid Earthquakes

(after Johnston, A. C., 1982)





## SECTION 3

### BEDROCK MOTION MODEL

In many engineering applications, earthquake excitations are usually represented by power spectral density functions (power spectra), acceleration time histories or response spectra. Earthquake motions can be generated by empirical approaches [22,23], semi-theoretical approaches [24–27] and theoretical approaches [28–33]. Due to the lack of strong-motion data in the central and eastern United States, a seismologically-based model is utilized to describe the horizontal bedrock motions at a site due to primarily shear waves generated from a seismic source. This model is centered on a power spectrum which is in turn developed from a seismologically-based Fourier amplitude spectrum. From the power spectrum, earthquake time histories and probability-based response spectra such as 84 percentile non-exceedance response spectra, can be generated directly.

#### 3.1 Fourier Amplitude Spectrum

Several seismologically-based Fourier amplitude spectra have been proposed [29,32,33]. The Fourier amplitude spectrum used in this study essentially follows the Boore and Atkinson approach [29] and is expressed as follows:

$$A(f) = C \times S(f) \times D(f) \times I(f) \quad (3.1)$$

where  $C$  is a scaling factor;  $S(f)$  is a source spectral function;  $D(f)$  is a diminution function; and  $I(f)$  is a shape filter.

##### 3.1.1 Source Spectral Function

The source spectral function  $S(f)$  is a frequency-domain representation of the seismic energy released by an earthquake. In this study, an  $\omega^2$  source spectrum of shear waves proposed by Brune [34,35] and Aki [36] is utilized. This source spectrum is a function of a single corner frequency  $f_0$  and seismic moment  $M_0$

$$S(f) = \frac{M_0}{1 + \left(\frac{f}{f_0}\right)^2} \quad (3.2)$$

The corner frequency  $f_0$  is related to the seismic moment  $M_0$  through shear wave velocity  $\beta$  and stress parameter  $\Delta\sigma$

$$f_0 = 4.9 \times 10^6 \beta \left( \frac{\Delta\sigma}{M_0} \right)^{\frac{1}{3}} \quad (3.3)$$

The seismic moment  $M_0$  is related to average displacement  $\bar{D}$  and fault rupture area  $A$  as follows:

$$M_0 = \mu A \bar{D} \quad (3.4)$$

where  $\mu$  is the modulus of rigidity in the source zone [37]. The equation relating moment magnitude  $M$  to seismic moment  $M_0$  established by Hanks and Kanamori [38] is

$$M = \frac{2}{3} \log M_0 - 10.7 \quad (3.5)$$

Since the moment magnitude  $M$  is most closely related to the physical characteristics of the seismic source, it is used to describe the size of earthquakes through out this study.

The stress parameter  $\Delta\sigma$  is a parameter describing the level of the source spectral function above the corner frequency  $f_0$ . For a fixed moment magnitude  $M$  and a constant shear wave velocity  $\beta$ , the corner frequency  $f_0$  in equation (3.3) varies with the stress parameter  $\Delta\sigma$ . The stress parameter  $\Delta\sigma$  proposed by Brune [34,35], Joyner [39], Atkinson [40], and Boore and Atkinson [29] is a constant and independent of earthquake magnitude while the stress parameter suggested by Nuttli [41] increases with magnitude. In this study, we adopt the constant stress parameter to predict the peak ground accelerations. Several values of  $\Delta\sigma$  have been proposed by Boore and Atkinson [29], Somerville and others [42], McGuire and others [31,43], and Nebelek and Suarez [44]. Among them, Boore and Atkinson [29], McGuire and others [31], and Somerville and others [42] concluded an average  $\Delta\sigma$  around 100 bars. Nebelek and Suarez [44], on the other hand, suggested a stress value as high as 670 bars for the 1983 Goodnow earthquake. Nevertheless, the most commonly accepted stress value for the eastern North America is 100 bars. Thus, the stress parameter  $\Delta\sigma$  for the New Madrid earthquakes is taken as 100 bars.

### 3.1.2 Scaling Factor

According to the scaling law suggested by Boore [28] and Joyner [39], the scaling factor  $C$  is a constant given by

$$C = \frac{\langle R_{\theta\phi} \rangle \cdot F \cdot V}{4\pi \cdot \rho \cdot \beta^3} \cdot \frac{1}{r} \quad (3.6)$$

where

$\langle R_{\theta\phi} \rangle$  = Radiation pattern

$F$  = Free surface effect

$V$  = Partition of a vector into horizontal components

$\beta$  = Continental crustal shear wave velocity

$\rho$  = Crustal density

$r$  = Hypocentral distance

$\langle R_{\theta\phi} \rangle$  is the radiation patterns correspond to different types of seismic waves over a range of azimuths ( $\theta$ ) and take-off angles ( $\phi$ ). For  $\phi$  and  $\theta$  averaged over the whole focal sphere, the shear-wave radiation pattern  $\langle R_{\theta\phi} \rangle$  is 0.55 [45].  $F$  is the amplification due to the free surface and is assumed as 2 [28,29].  $V$  is the factor which accounts for the partition of a vector into horizontal components and is chosen as  $1/\sqrt{2}$ .

The shear wave velocity  $\beta$  is the average crustal shear wave velocity near the seismic source. Based on the hypocentral locations of the instrumentally recorded microearthquakes in the New Madrid seismic zone, the focal depths normally range from 5 to 20 kilometers below the surface where the granitic basement rock of the upper and middle continental crusts are found. In this study, a continental crustal shear wave velocity  $\beta$  of 3.5 km/sec is used for an average focal depth of 10 km. The average crustal density  $\rho$  of continental crust at this focal depth is taken as  $2.7g/cm^3$ .

The hypocentral distance  $r$  is the distance measured from the focus of an earthquake to the surface at which a selected site is located. The term  $1/r$  in equation (3.6) accounts for the diminishing of the source spectrum as a result of body-wave geometric spreading. At hypocentral distances greater than 100 kilometers,  $r$  is replaced by  $\sqrt{r_x r}$ , where  $r_x$  indicates

a distance beyond which the dominant ground-motion signal can be better described by the  $L_g$  waves than shear waves [29,31,46]. In this study,  $r_z$  is chosen as 100 kilometers.

### 3.1.3 Diminution Function

The diminution function  $D(f)$  represents the anelastic attenuation which accounts for the damping of the earth's crust and a sharp decrease of acceleration spectra above some cut-off frequency. These phenomena are expressed by the following equation

$$D(f) = \exp\left[\frac{-\pi \cdot f \cdot r}{Q(f) \cdot \beta}\right] \cdot P(f, f_m) \quad (3.7)$$

where

$Q(f)$  = Frequency-dependent quality factor

$P(f, f_m)$  = High-cut filter

The exponential term in equation (3.7) accounts for the path attenuation. The quality factor  $Q(f)$  is shown in equation (2.1) as suggested by Dwyer and others [19]. The high-cut filter  $P(f, f_m)$  accounts for the observation that the acceleration spectra often show a sharp decrease above some cut-off frequency  $f_m$  which cannot be attributed to the path attenuation. In this study, a Butterworth filter with a cut-off frequency  $f_m$  set at 40 Hz is used as the high-cut filter  $P(f, f_m)$ :

$$P(f, f_m) = \left[1 + \left(\frac{f}{f_m}\right)^8\right]^{-1/2} \quad (3.8)$$

### 3.1.4 Shape Filter

The shape filter  $I(f)$  is used to shape the source spectral function for a particular type of earthquake motion of interest. For acceleration, the filter function is given as

$$I(f) = (2\pi f)^2 \quad (3.9)$$

The essential parameters used to compute the Fourier amplitude spectra of bedrock acceleration with moment magnitude  $M = 7.5$  and epicentral distance  $R = 50$  km are summarized in Table 3-I. The resulting Fourier amplitude spectrum is presented in figure 3-1.

**TABLE 3-I SUMMARY OF PARAMETERS**

	<u>SYMBOL</u>	<u>VALUE</u>
MOMENT MAGNITUDE	$M$	7.5
EPICENTRAL DISTANCE	$R$	50 km
RADIATION PATTERN	$\langle R_{\theta\phi} \rangle$	0.55
HORIZONTAL COMPONENT	$V$	0.71
SHEAR WAVE VELOCITY	$\beta$	3.5km/sec
SOURCE ROCK DENSITY	$\rho$	2.7g/cm <sup>3</sup>
QUALITY FACTOR	$Q(f)$	1500f <sup>0.4</sup>
STRESS PARAMETER	$\Delta\sigma$	100bars
CUT-OFF FREQUENCY	$f_m$	40.0Hz

FOURIER AMPLITUDE SPECTRUM

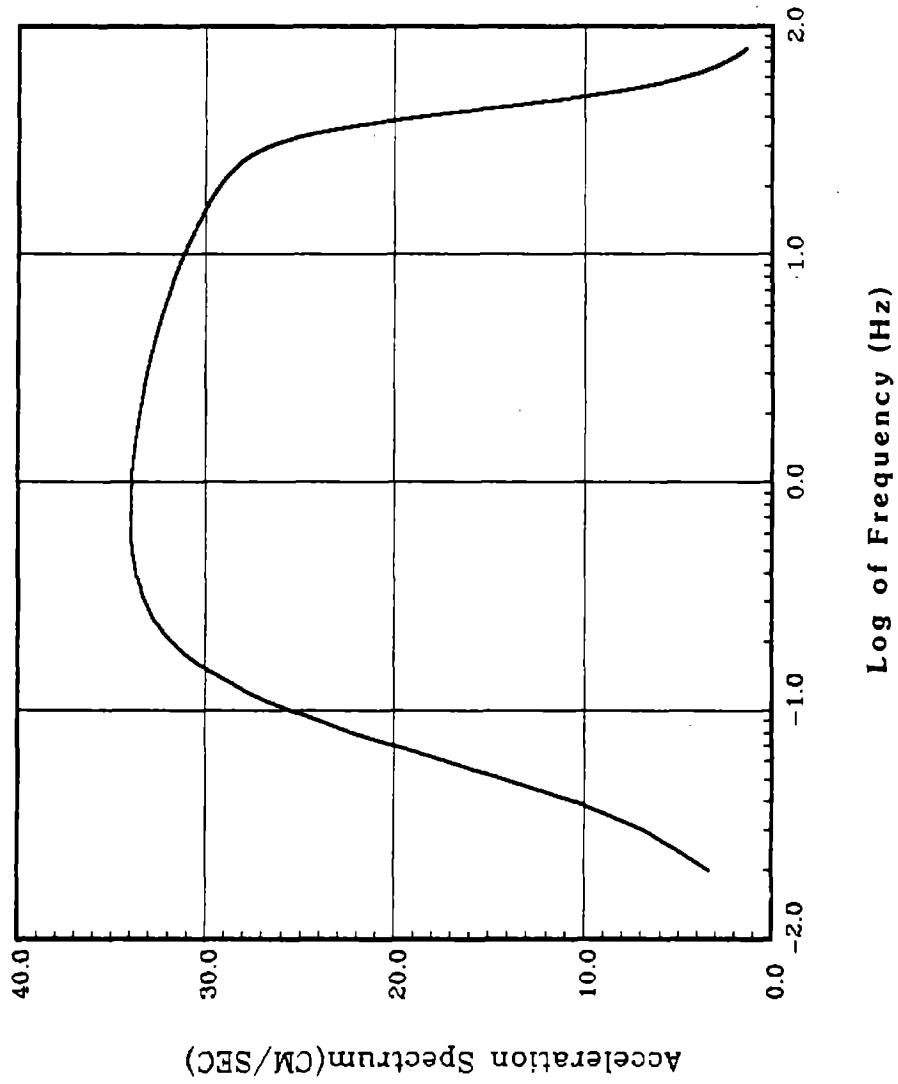


Figure 3-1 Fourier Amplitude Spectrum ( $M = 7.5$  and  $R = 50$  km)

### 3.2 Power Spectral Density Function

The power spectrum of an earthquake can be calculated from the Fourier amplitude spectrum. An earthquake accelerogram generally shows a build-up segment followed by a strong motion segment which is in turn followed by a decay segment. Moayyad and Mohraz [47] found that the frequency content of earthquake accelerograms is approximately constant during the strong motion segment. Thus, the strong motion segment of an acceleration time history is considered as a stationary random process and its one-sided power spectral density function  $S_{aa}(f)$  is

$$S_{aa}(f) = \frac{2}{T} |A(f)|^2 \quad (3.10)$$

where  $A(f)$  is the Fourier amplitude spectrum as in equation (3.1) and  $T$  is the duration of the strong motion. In this study, strong motion duration  $T$  is chosen as the source duration which is equal to the reciprocal of the corner frequency  $f_0$  [48,49].

$$T = 1/f_0 \quad (3.11)$$

The power spectrum of an earthquake of moment magnitude  $M = 7.5$  and epicentral distance  $R = 50$  km is plotted in figure 3-2.

### 3.3 Time Histories

In this study, the method proposed by Shinozuka [50,51] is employed for generating synthetic earthquake time histories. The stationary acceleration time histories  $a_s(t)$  can be generated from the equation below

$$a_s(t) = \sqrt{2} \sum_{k=1}^N \sqrt{S_{aa}(\omega_k) \Delta\omega} \cdot \cos(2\pi\omega_k t + \phi_k) \quad (3.12)$$

where

$S_{aa}(\omega_k)$  = One-sided earthquake power spectrum

$N$  = Number of frequency intervals

$\Delta\omega$  = Frequency increment

$\omega_k = k\Delta\omega$

$\phi_k$  = Random phase angles uniformly distributed between 0 and  $2\pi$

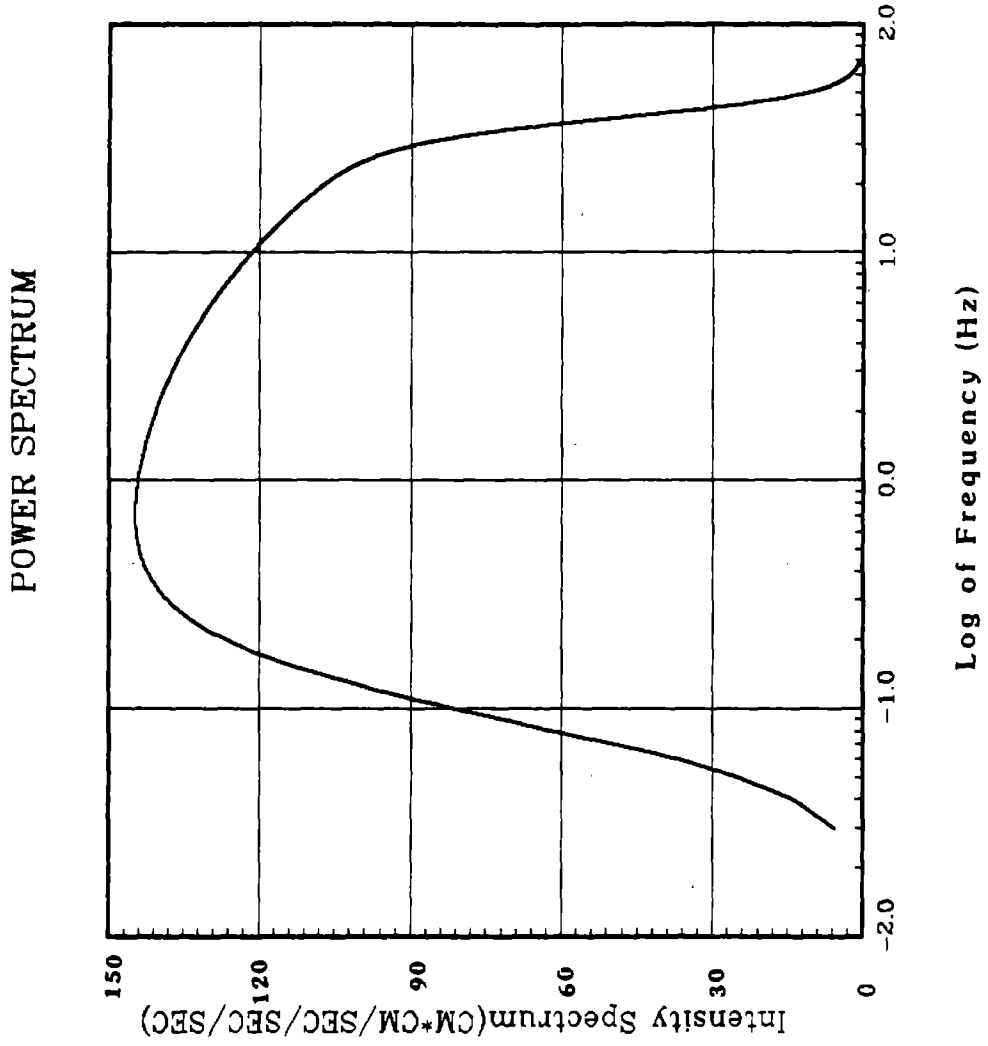


**Figure 3-2 Power Spectrum (M = 7.5 and R = 50 km)**



The nonstationary acceleration time histories  $a(t)$  can be obtained from the multiplication of an envelope function  $W(t)$ .

$$a(t) = a_s(t) \cdot W(t) \quad (3.13)$$

In this study, the envelope function  $W(t)$  is comprised of three segments : (1) a parabolically increased segment simulating the initial rise part of the accelerogram and its duration is chosen as one fifth of  $T$ ; (2) a constant segment representing the strong motion portion of an earthquake excitation and has a duration equals to  $T$ ; and (3) a linearly decayed segment extending four-fifth of  $T$ . Thus, the total duration is  $2T$ . It is noted that real earthquake records are commonly observed with long coda durations, however, in most engineering applications the coda durations are considered unimportant. The total duration used in this study is, therefore, adequate for engineering applications. The envelope function for an earthquake of  $M = 7.5$  is shown in figure 3-3. The source duration computed from equation (3.11) is 16 seconds and the total duration is 32 seconds. From equations (3.12) and (3.13), a sample of accelerogram of  $M = 7.5$  and  $R = 50$  km is generated and displayed in figure 3-3.

### 3.4 Probability-Based Response Spectra

Conventional methods for generating response spectra are through earthquake time histories. These methods, however, are tedious and time-consuming. In this study, a more efficient method based on the random vibration theory is adopted to compute the response spectra directly from the power spectrum [52]. Furthermore, the response spectra computed by this approach has statistical meaning such as the mean response spectra or 90 percentile non-exceedance response spectra.

A response spectrum is a representation of the maximum response (displacement, velocity, acceleration, etc.) to a specified input earthquake for all possible simple oscillators. The equation of motion for a simple oscillator with natural frequency  $\omega_0$  and damping ratio  $\zeta$  is

$$\ddot{x} + 2\zeta\omega_0\dot{x} + \omega_0^2x = -a(t) \quad (3.14)$$

where  $x(\omega_0, t)$  is the relative displacement and  $a(t)$  is the input earthquake acceleration time history. For zero initial condition, the relative displacement  $x(\omega_0, t)$  obtained from

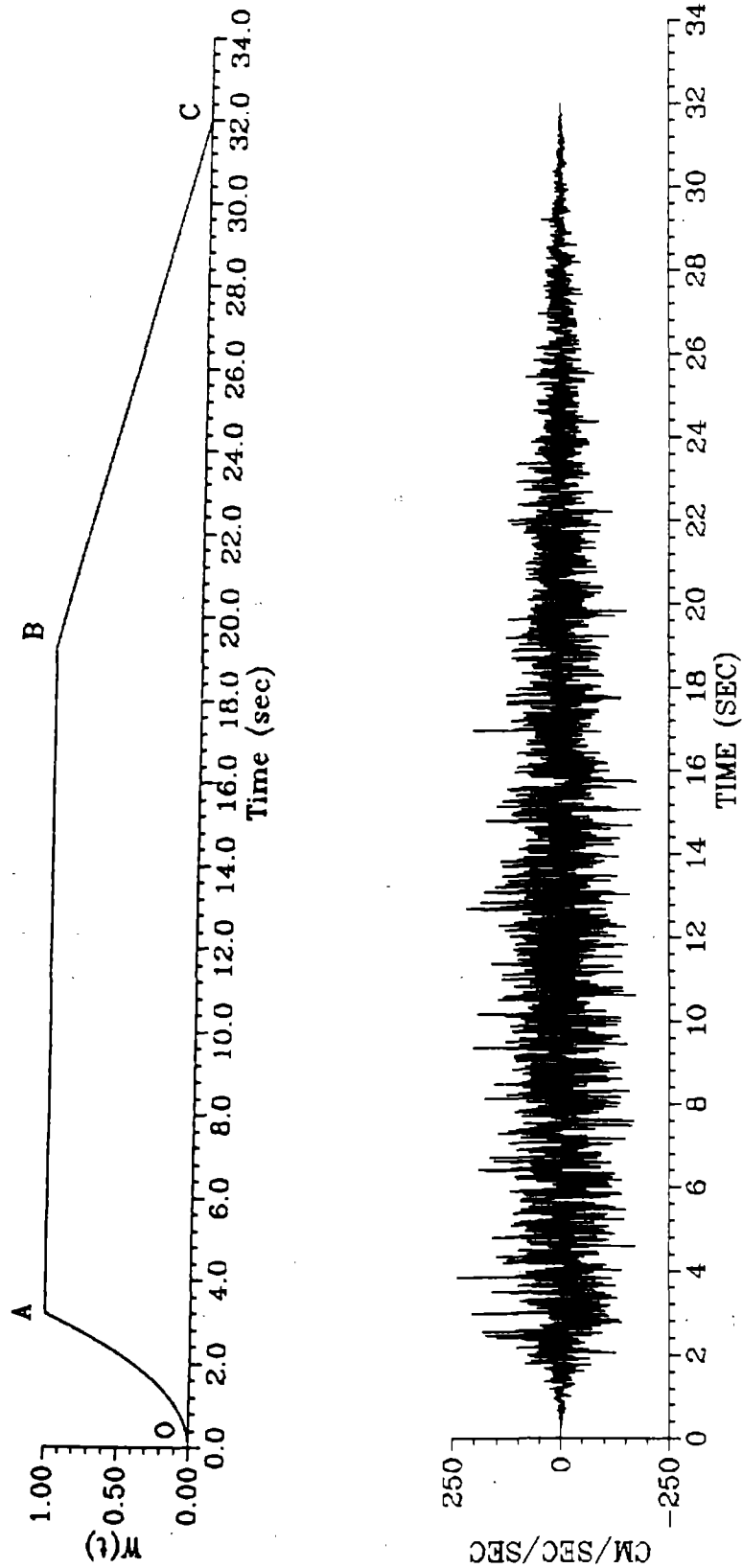


Figure 3-3 Example of Envelope Function and Earthquake Time History

equation (3.14) is

$$x(\omega_0, t) = \frac{-1}{\omega_d} \int_0^t a(\tau) \exp[-\zeta\omega_0(t - \tau)] \sin[\omega_d(t - \tau)] d\tau \quad (3.15)$$

where,  $\omega_d = \omega_0(1 - \zeta^2)^{1/2}$ . For a given frequency  $\omega_0$ , the ordinate of the relative displacement response spectrum  $R_d$  is the maximum absolute value of  $x(\omega_0, t)$ , that is

$$R_d = \max |x(\omega_0, t)| \quad (3.16)$$

Assuming that an earthquake is a stationary Gaussian process with mean zero and one-sided power spectrum  $S_{aa}(\omega)$ , the relative displacement response  $x(\omega_0, t)$  of a simple oscillator with natural frequency  $\omega_0$ , is also a stationary Gaussian process with mean zero and the power spectrum  $S_x(\omega)$ .

$$S_x(\omega) = |H(\omega)|^2 S_{aa}(\omega), \quad (3.17)$$

where  $H(\omega)$  is the complex frequency response function

$$H(\omega) = \frac{1}{(\omega_0^2 - \omega^2) + 2i\zeta\omega\omega_0} \quad (3.18)$$

with  $i = \sqrt{-1}$ . As defined in equation (3.16),  $R_d$  is the maximum absolute value of  $x(\omega_0, t)$ . From Appendix A, the mean value  $\bar{R}_d$  can be determined from

$$\bar{R}_d = p_m \cdot \sigma_x \quad (3.19)$$

where  $p_m$  is the mean peak factor and  $\sigma_x$  is the standard deviation of the displacement response. The mean pseudo-acceleration response spectrum  $\bar{R}_a$  can be computed from

$$\bar{R}_a = \omega_0^2 \bar{R}_d. \quad (3.20)$$

The mean response spectra for earthquakes of several different moment magnitudes at  $R = 100$  km are shown in figure 3-4. Variation of peak spectral accelerations with respect to moment magnitudes can be seen from the figure.

# MEAN RESPONSE SPECTRA

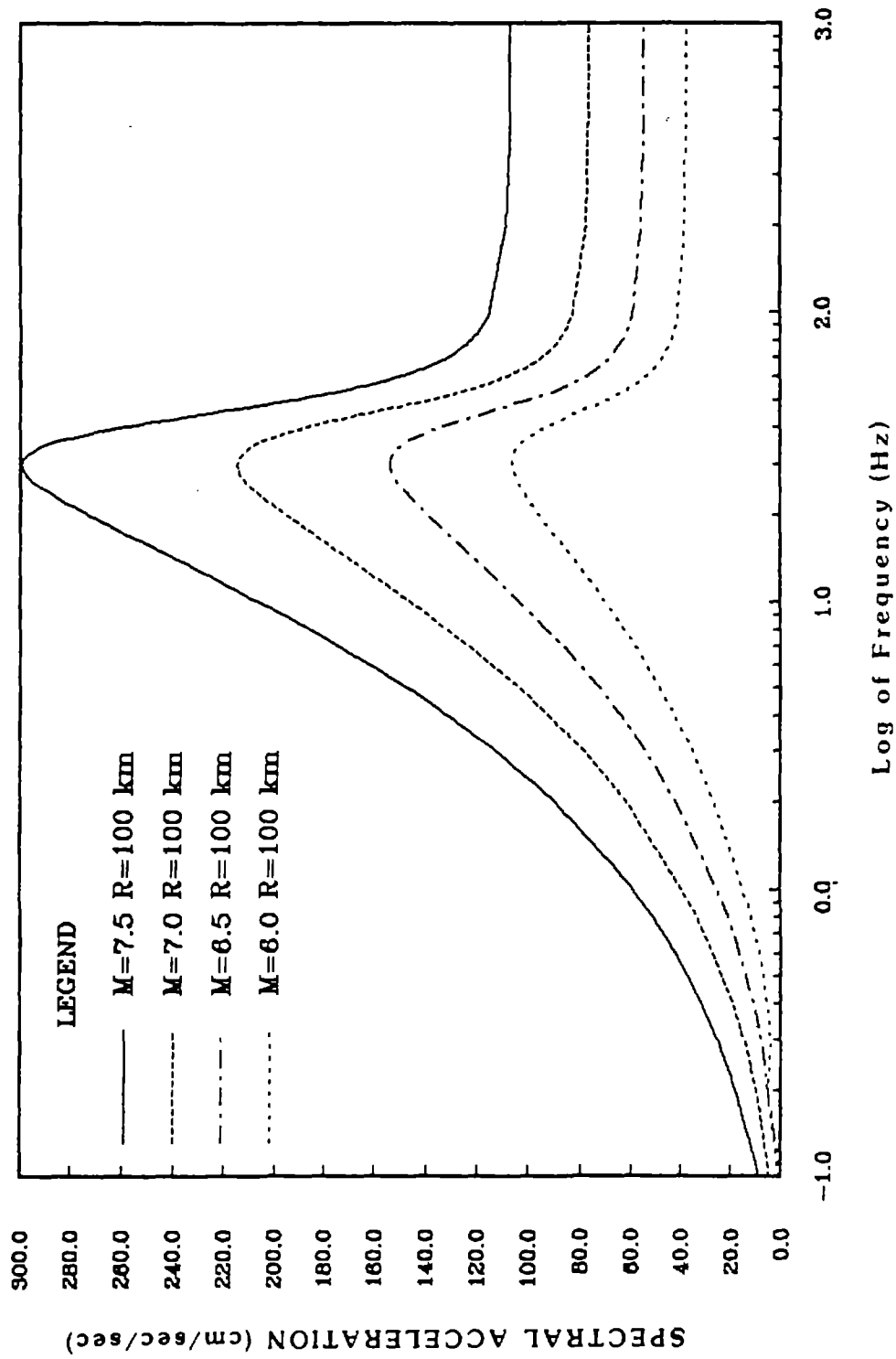


Figure 3-4 Mean Bedrock Response Spectra of Various Moment Magnitudes

### 3.5 Comments on Parameter Uncertainties

The seismologically-based model for the horizontal bedrock accelerations is defined by several parameters as described in Section 3. Some parameters such as source rock density  $\rho$  and shear wave velocity  $\beta$  appear to have less influence on the resulting bedrock accelerations. On the other hand, parameters such as quality factor  $Q(f)$ , stress parameter  $\Delta\sigma$ , and cut-off frequency  $f_m$  seem to have significant effects on the bedrock accelerations. The quality factor expressed in equation (2.1) is used in this study. Modeling uncertainty is accounted for if different equations for the quality factor e.g., equations (2.2) and (2.3) are also used. Furthermore, the selection of values other than those used in this study for stress parameter and cut-off frequency will cover the random uncertainty. In this study, the most commonly accepted value of each parameter for the study region is utilized. The random and modeling uncertainties are not included because of the lack of strong motion data to quantify these uncertainties. This is a topic needs to be studied in the future when more strong motion data are available.



## SECTION 4

### PEAK BEDROCK ACCELERATIONS IN MEMPHIS AREA

The seismic hazard in Memphis and Shelby County, Tennessee is entirely dominated by earthquakes in the New Madrid seismic zone (figure 1-1). In this study, the peak values of bedrock accelerations in Memphis and Shelby County are computed for two large New Madrid earthquakes of  $M = 7.5$  and  $6.5$ . The moment magnitude 7.5 earthquake represents a major event to be considered for the seismic risk assessment and emergency response planning. On the other hand, the moment magnitude 6.5 earthquake is known to have significantly high probability of occurrence between now and early next century [53].

For the purpose of constructing contour maps, a grid system consists of rectangular cells with equal size of 30 seconds in both latitude and longitude is selected [54]. As a result, over three thousand grid points within Memphis and Shelby County region are created (figure 4-1).

#### 4.1 Estimation of Peak Bedrock Accelerations

The peak value  $A_p$  of a bedrock acceleration time history  $a(t)$  can be expressed as

$$A_p = \max|a(t)| \quad (4.1)$$

The mean value  $\bar{A}_p$  and standard deviation  $\sigma_{A_p}$  of the peak values can be determined from the random process theory as shown in Appendix A.

$$\bar{A}_p = p_m \cdot \sigma_a \quad (4.2)$$

$$\sigma_{A_p} = q \cdot \sigma_a \quad (4.3)$$

where  $\sigma_a$ ,  $p_m$  and  $q$  can be determined from equations (A.1), (A.7) and (A.8), respectively, in Appendix A.

#### 4.2 A Marked Tree Event

Marked Tree, Arkansas is located near the end of the southern New Madrid seismic zone (figure 4-2). On January 4, 1843, an  $m_b = 6.0$  earthquake occurred at this location [55].

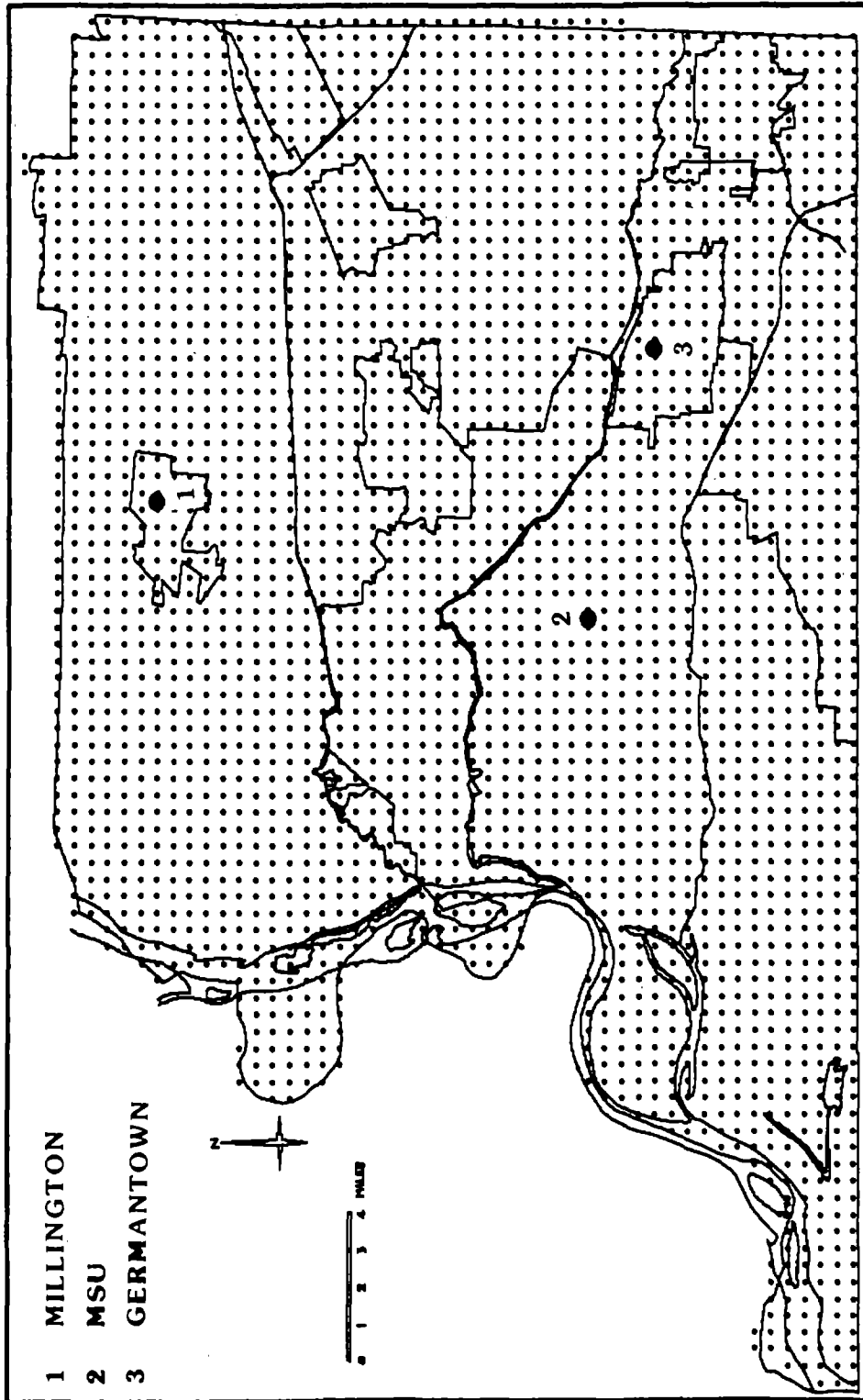


Figure 4-1 Grid Points in Shelby County



# NEW MADRID SEISMIC ZONE

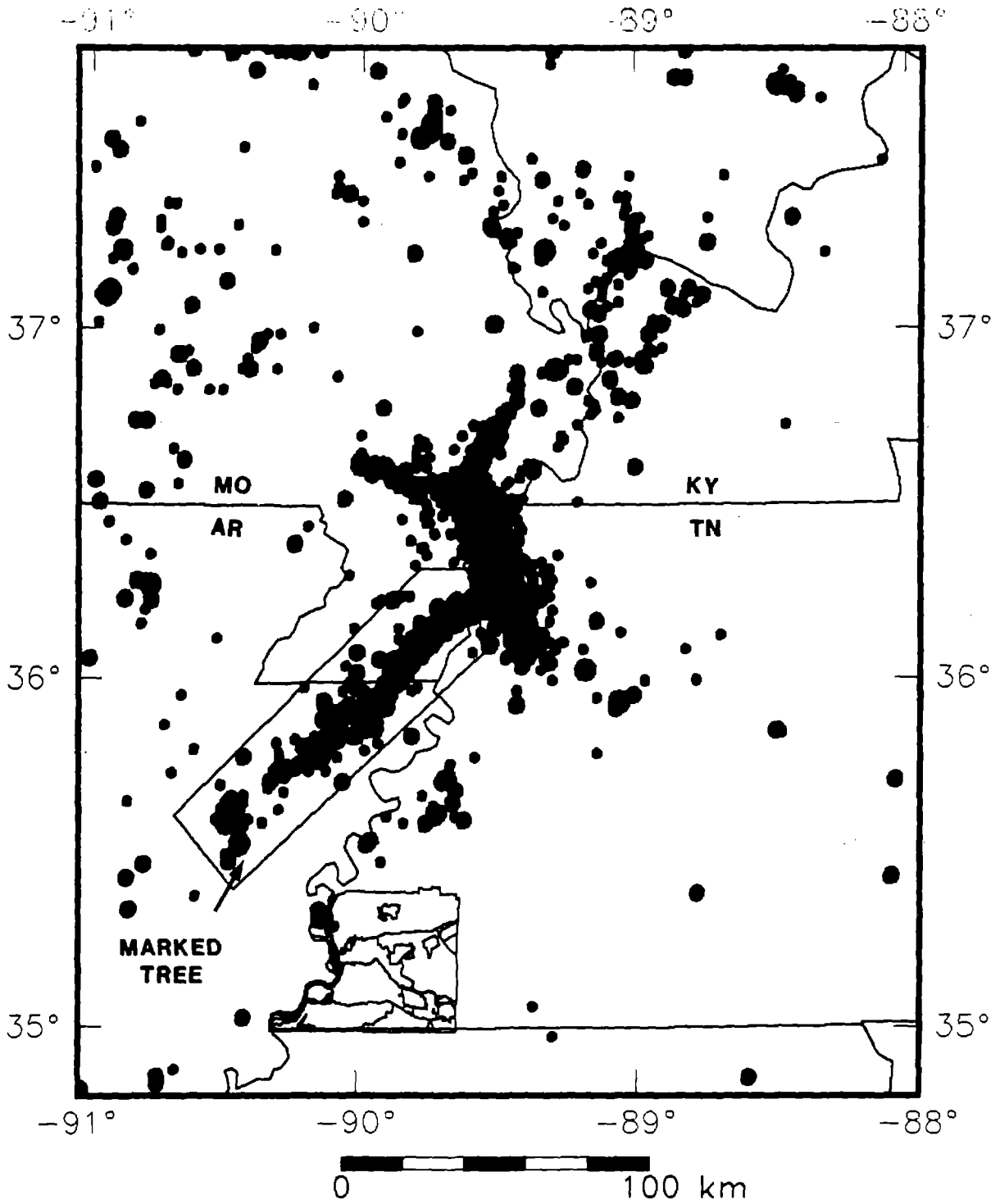


Figure 4-2 Boundary of the Southern New Madrid Seismic Zone

Thus, in this study, a single source at Marked Tree is first assumed to estimate the peak values through out the county. Table 4-I shows the mean peak values and coefficients of variation (COV) of three selected sites, Memphis State University (MSU), Millington and Germantown resulting from a Marked Tree event of  $M = 7.5$ . It can be seen that COV of the peak accelerations are generally less than 10 percents. The variation of peak acceleration is thus negligible and only the mean values of peak accelerations are used to construct the contour maps. The contour maps of mean peak values for the  $M = 7.5$  and 6.5 events are presented in figures 4-3 and 4-4, respectively.

### 4.3 Southern Segment of NMSZ

Memphis and Shelby county are located southeast of the NMSZ. If an earthquake occurs in the southern segment of the NMSZ, it may have a significant impact on Memphis and Shelby County. Since we cannot predict where the next New Madrid earthquake will occur, we assume that an earthquake may occur anywhere in the southern NMSZ. The boundary of the southern NMSZ is defined in figure 4-2. A grid system is applied to the southern NMSZ and results in 155 source points. In order to evaluate the peak values of a site due to the southern NMSZ, the peak accelerations from all 155 source points are computed using equation (4.2). From these 155 peak values, the mean, standard deviation and maximum values are determined. For the three sites, Memphis State University (MSU), Millington and Germantown, these values for an  $M = 7.5$  earthquake are tabulated in table 4-II. It can be seen that the mean plus one standard deviation value is very close to those obtained from the Marked Tree event. For an  $M = 7.5$  event, the contour maps for the mean, mean plus one standard deviation and maximum values are shown in figures 4-5, 4-6 and 4-7, respectively. The corresponding contour maps for an  $M = 6.5$  event are shown in figure 4-8, 4-9 and 4-10, respectively.

**TABLE 4-I Marked Tree Event  $M = 7.5$**

	<u>MILLINGTON</u>	<u>MSU</u>	<u>GERMANTOWN</u>
R	59km	66km	78km
MEAN	0.21g	0.18g	0.15g
SD	0.019g	0.016g	0.014g
COV	0.09	0.09	0.09

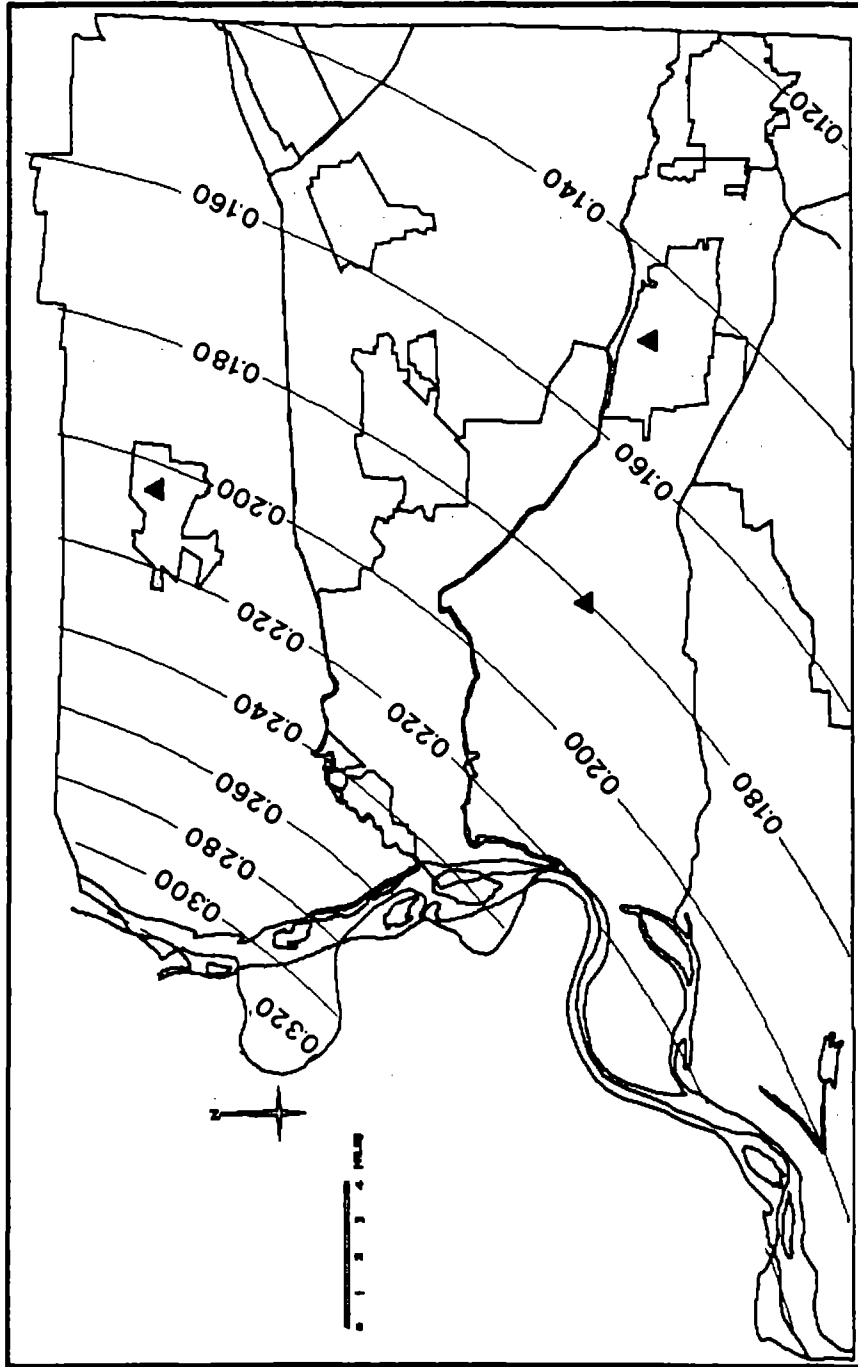


Figure 4-3 Contour Map of Mean Peak Accelerations ( $M = 7.5$ , Marked Tree Event)

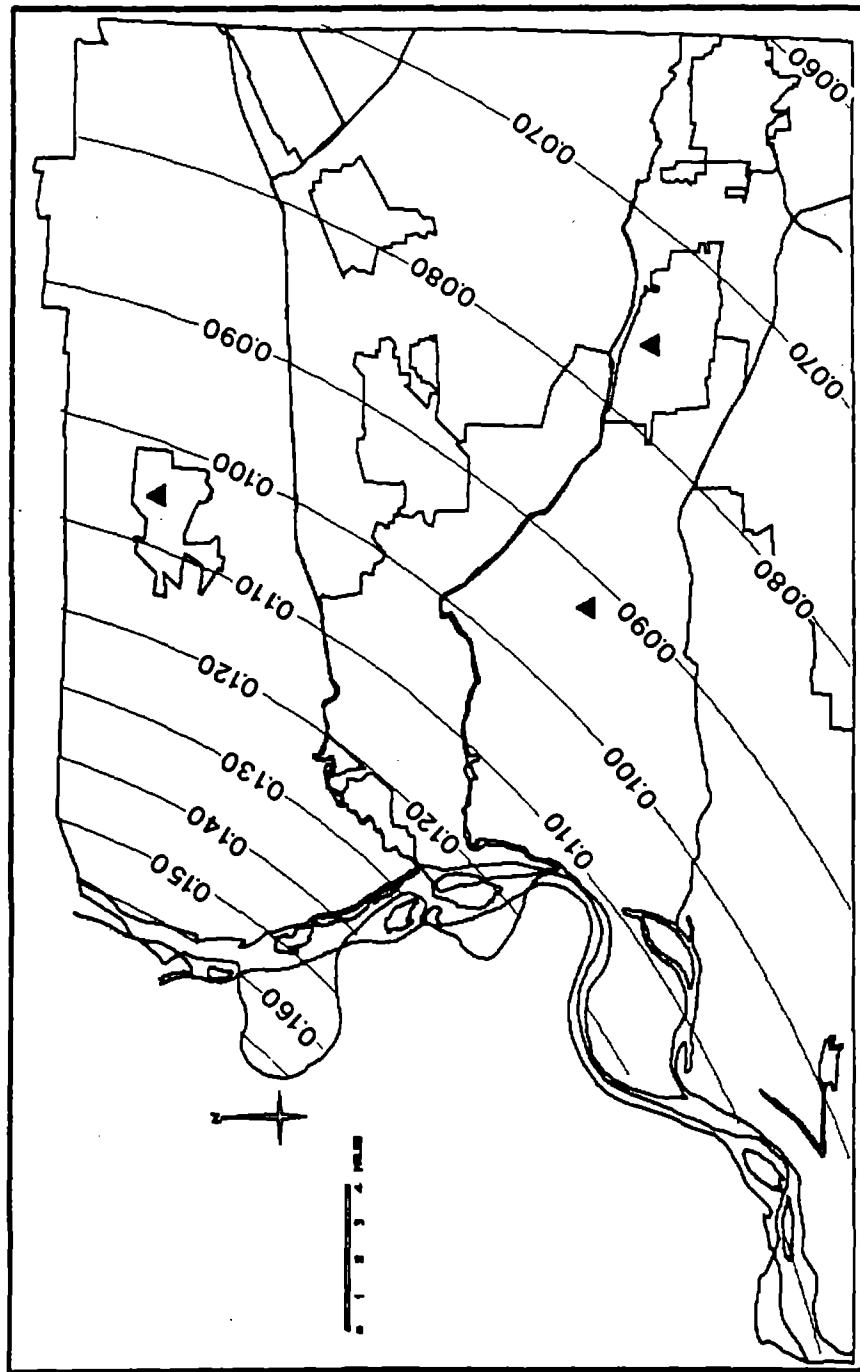


Figure 4-4 Contour Map of Mean Peak Accelerations ( $M = 6.5$ , Marked Tree Event)

**TABLE 4-II Distribution of Peak Values (Southern NMSZ, M = 7.5)**

	<u>MILLINGTON</u>	<u>MSU</u>	<u>GERMANTOWN</u>
MEAN	0.18g	0.14g	0.12g
SD	0.05g	0.04g	0.03g
MEAN + SD	0.23g	0.18g	0.15g
MAXIMUM	0.31g	0.22g	0.18g

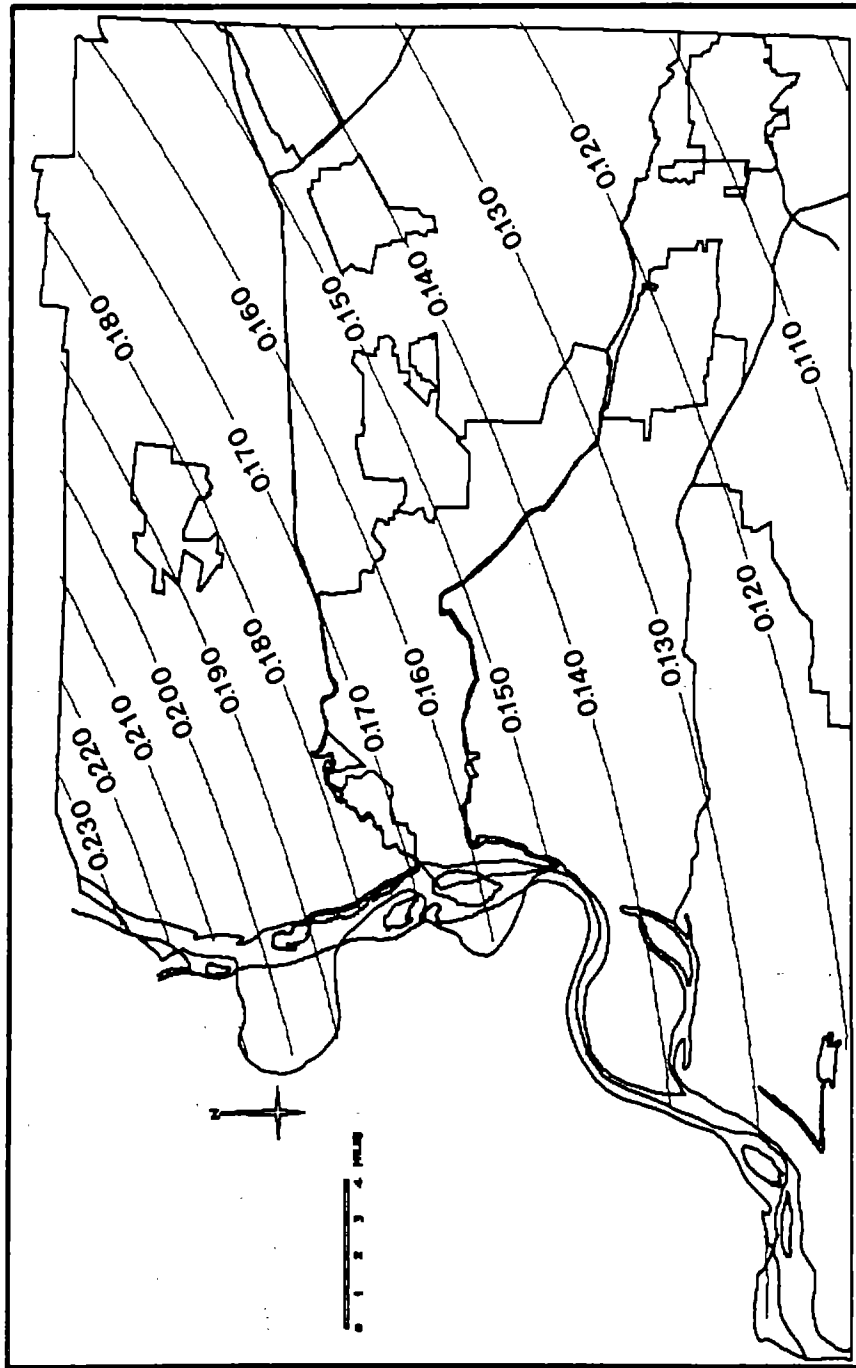


Figure 4-5 Contour Map of Mean Peak Accelerations ( $M = 7.5$ , Southern NMSZ)

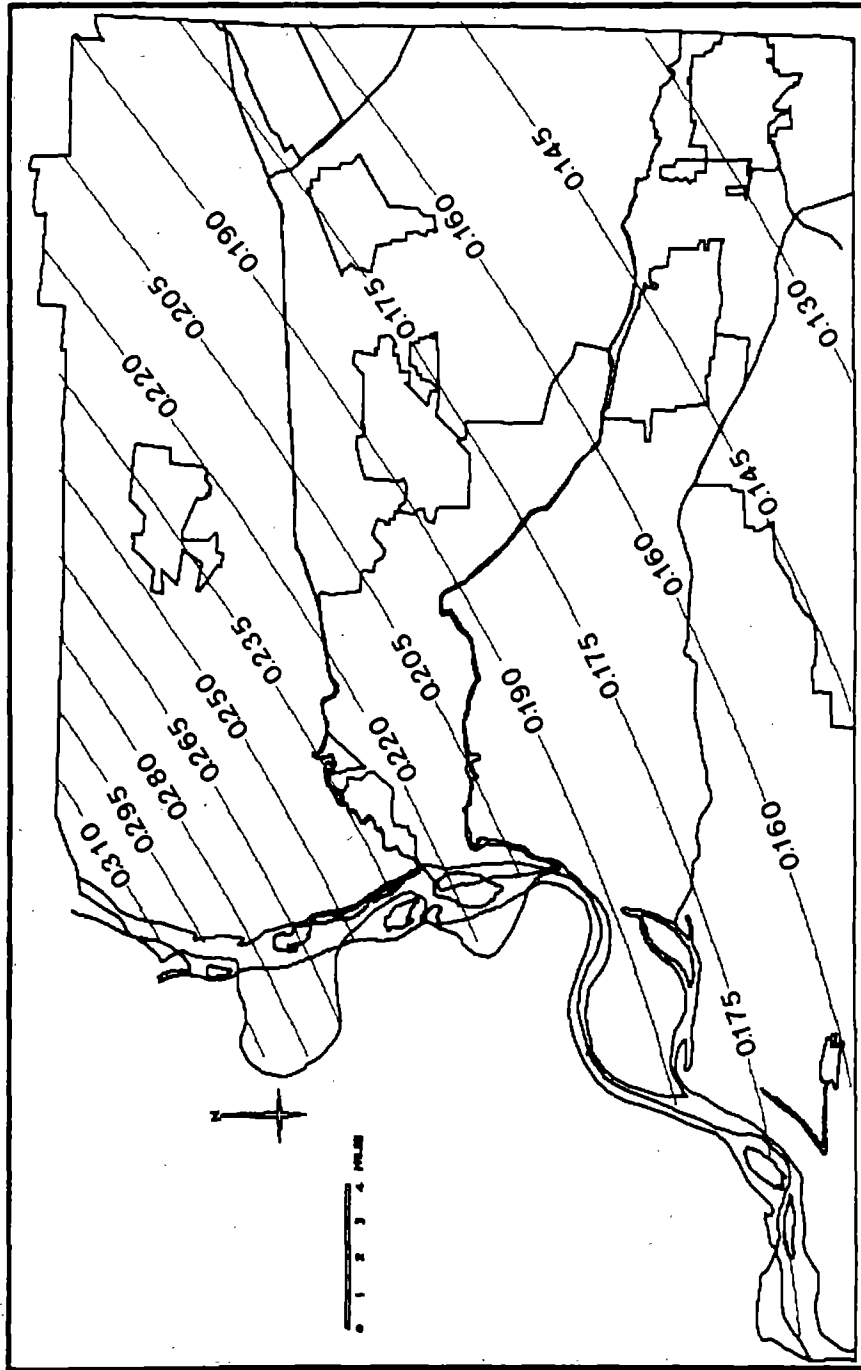


Figure 4-6 Contour Map of Mean + S.D. Accelerations ( $M = 7.5$ , Southern NMSZ)



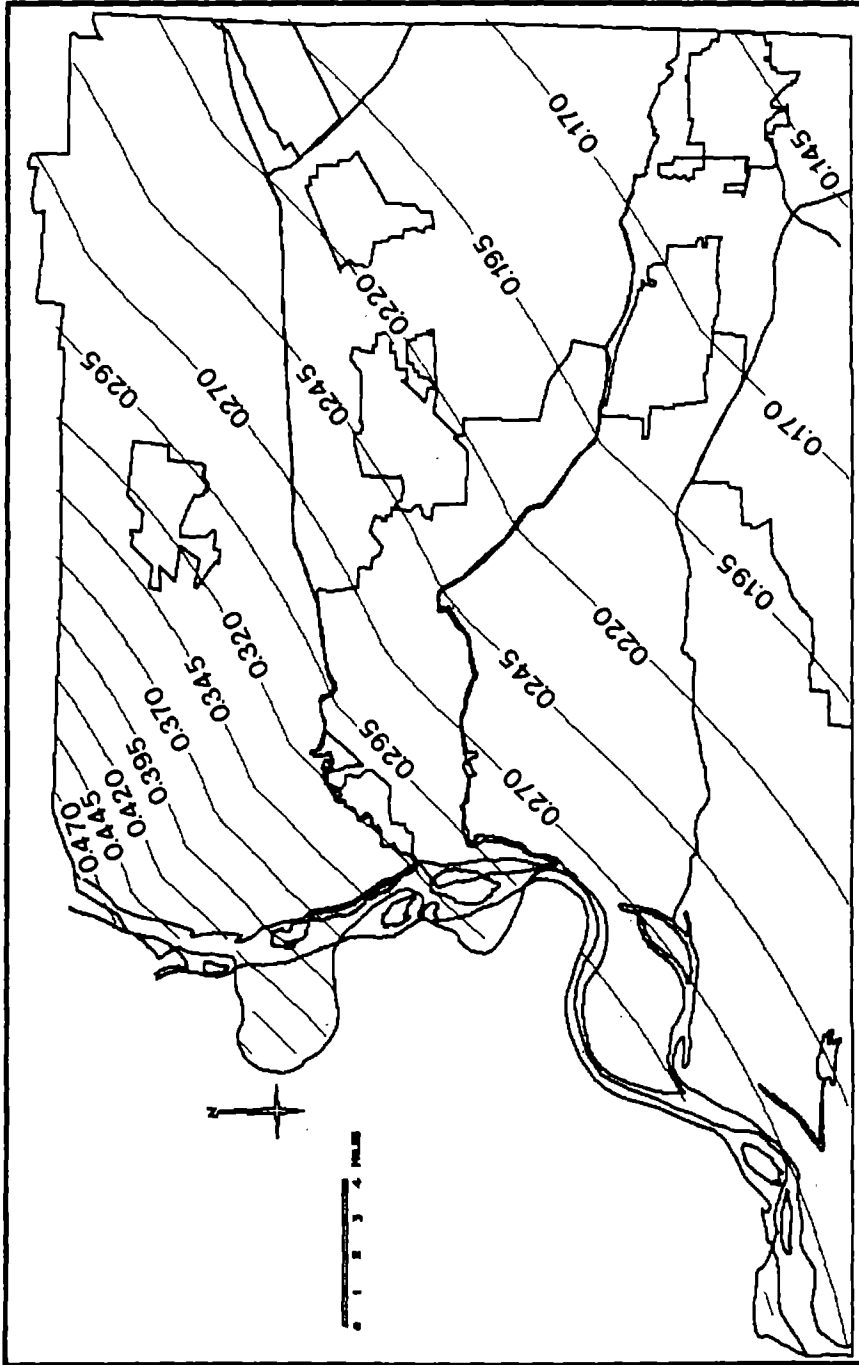


Figure 4-7 Contour Map of Maximum Accelerations (M = 7.5, Southern NMSZ)

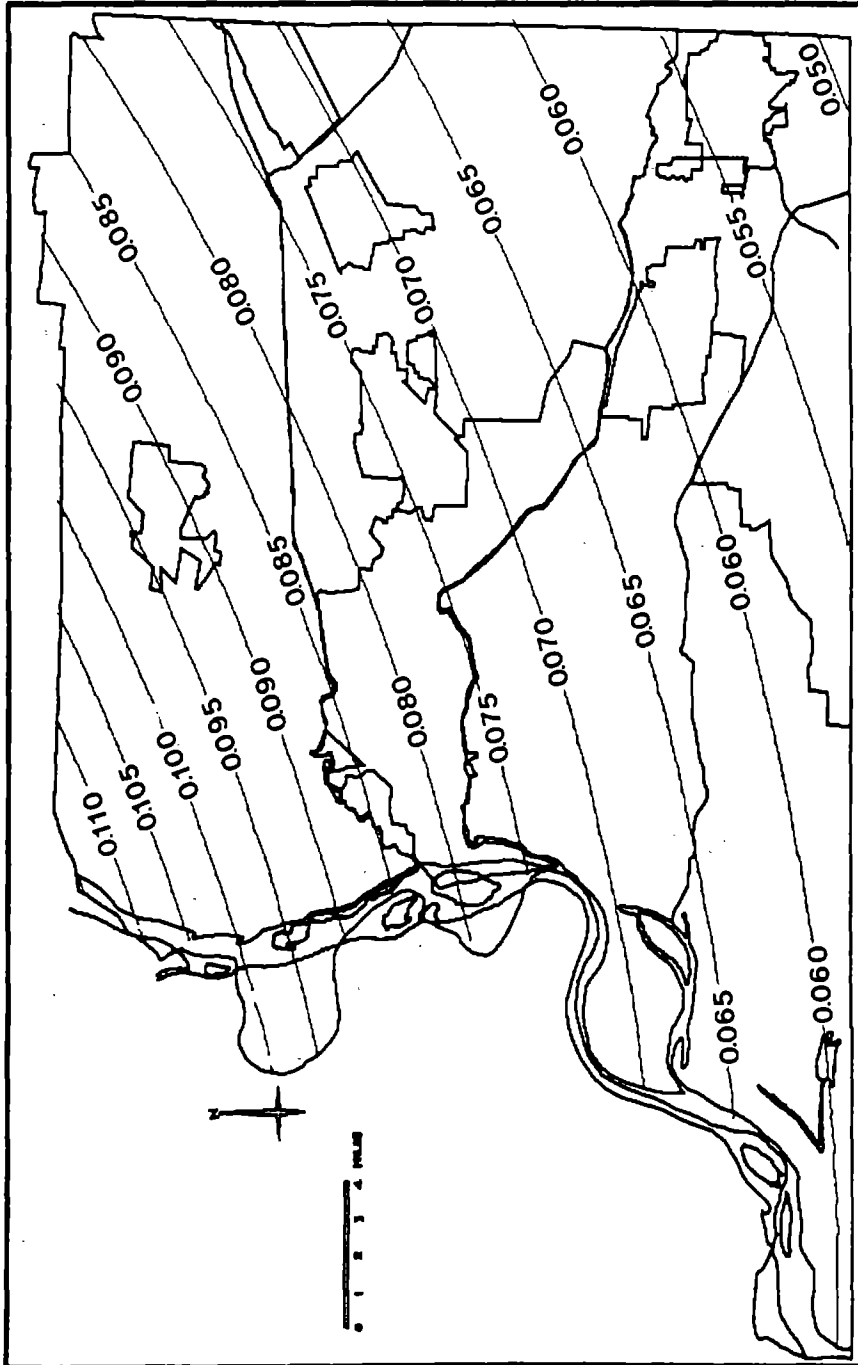


Figure 4-8 Contour Map of Mean Peak Accelerations ( $M = 6.5$ , Southern NMSZ)

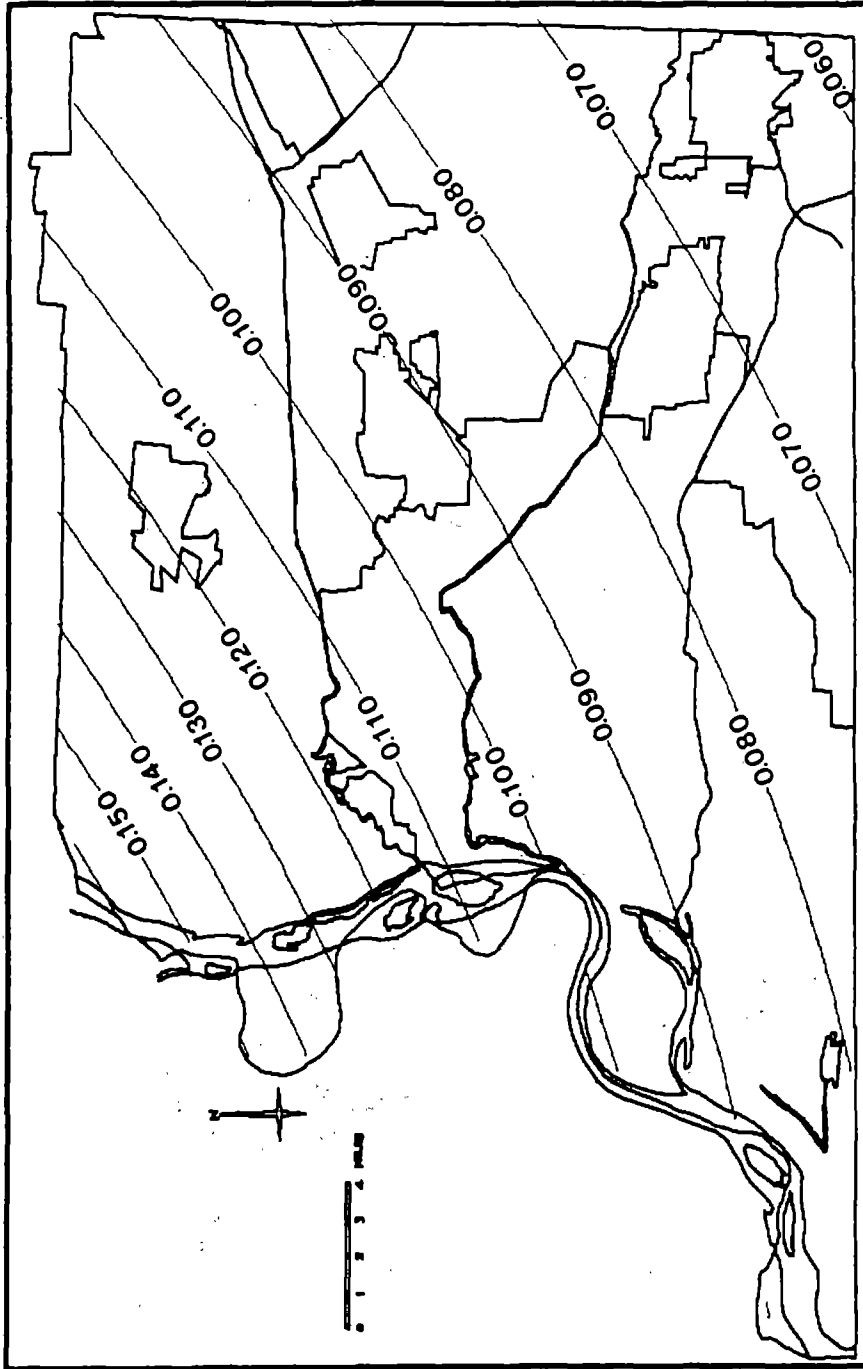


Figure 4-9 Contour Map of Mean + S.D. Accelerations (M = 6.5, Southern NMSZ)

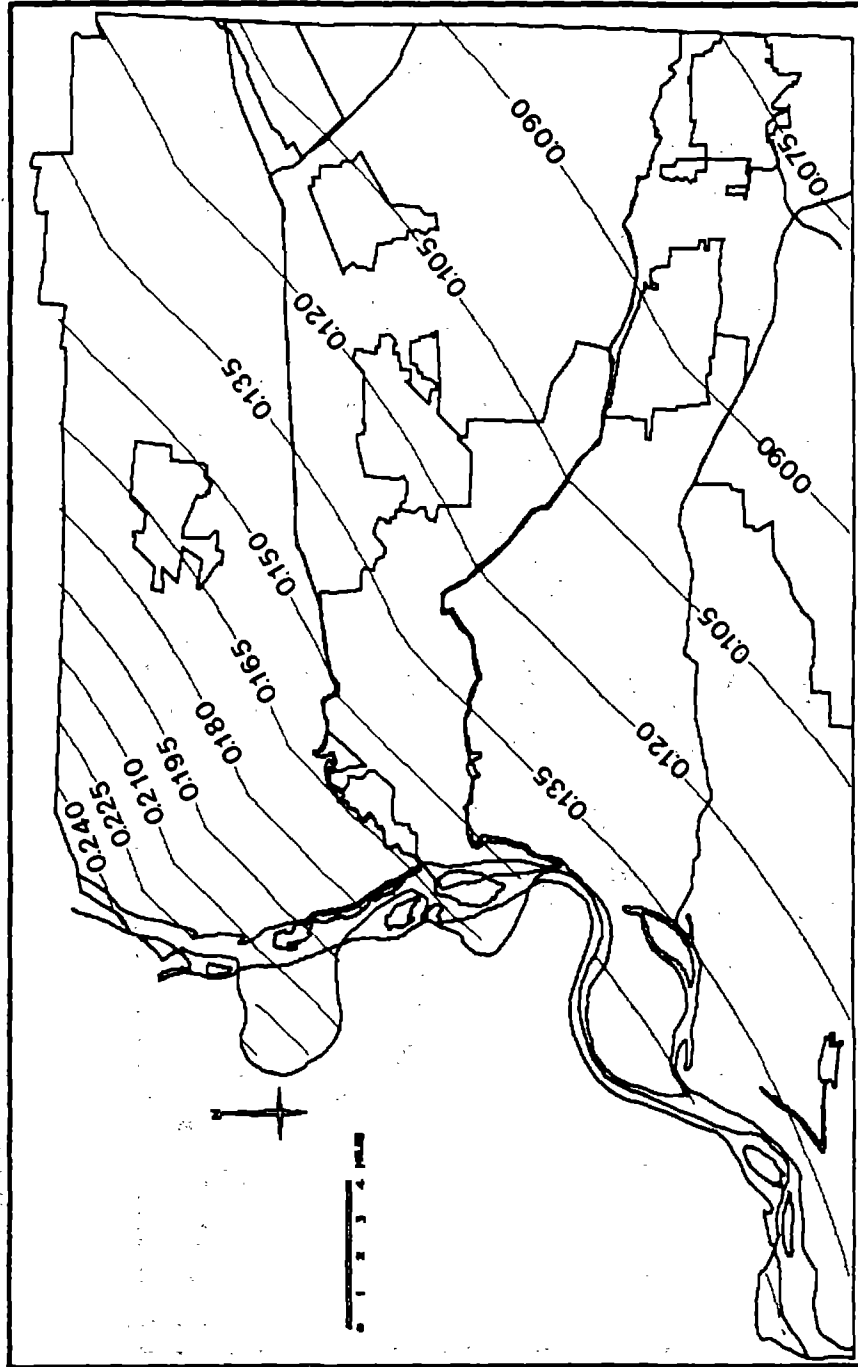


Figure 4-10 Contour Map of Maximum Accelerations ( $M = 6.5$ , Southern NMSZ)

## SECTION 5

### CONCLUSIONS

Memphis and Shelby County are geographically close to the southern segment of the New Madrid seismic zone (NMSZ). The NMSZ is being regarded by seismologists and earthquake engineers as the most hazardous zone in the eastern United States. Estimating the characteristics of seismic ground motions induced by large New Madrid earthquakes is an essential task for earthquake resistant design of structures and seismic risk assessment studies. In many engineering applications, earthquake excitations are usually represented by power spectra, time histories or response spectra. Making these quantitative estimates is quite challenging due to the lack of strong motion data in the New Madrid region.

In this study, a seismologically-based model is utilized to describe the horizontal bedrock motions at a site due to primarily shear waves generated from a seismic source. This model is centered on a power spectrum which is in turn developed from a seismologically-based Fourier amplitude spectrum. From the power spectrum, earthquake time histories and probability-based response spectra can be generated directly. As an example, the Fourier amplitude and power spectra, and an acceleration time history are generated for a New Madrid earthquake of moment magnitude  $M = 7.5$  and epicentral distance  $R = 50$  km. The mean response spectra corresponding to various  $M$  are also generated.

The power spectrum generated in this study can be used to estimate the peak value of earthquake accelerations based on the extreme value distribution of a random process. The peak values of bedrock accelerations for Memphis and Shelby County are computed for two New Madrid earthquakes of  $M = 7.5$  and  $6.5$ . Two cases of seismic sources are considered: (1) a single source at Marked Tree, Arkansas, and (2) the southern segment of the NMSZ. The results are presented in contour maps and are very useful for seismic risk assessment studies such as the Seismic Risk Assessment of Memphis Water Delivery System project.

The effects of soil conditions on earthquake ground motions have been well demonstrated by many actual earthquakes such as the 1964 Niigata earthquake, the 1967 Caracas earthquake, and the 1985 Mexico earthquake. Bedrock motions can be greatly modified, both

in amplitude and frequency characteristics, as seismic waves transmit through some overlying soil deposits. Memphis and Shelby County are located in the Mississippi embayment where relatively unconsolidated soils up to 3,000 feet thick are deposited. A recent study by Hwang and others [56] has demonstrated that the soil conditions in Memphis area have profound effects on earthquake ground motions. It is to be noticed that all the results presented in this report are pertinent to bedrock accelerations in Memphis and Shelby County. The subsurface conditions of Memphis and Shelby County have been established based on about 8,500 existing boring logs [54]. An effort is being carried out to study the effects of soil conditions on earthquake ground motions in the entire Memphis area.

## SECTION 6

### REFERENCES

1. Ervin, C. P., and McGinnis, L. D., "Reelfoot Rift - Reactivated Precursor to the Mississippi Embayment," *Bulletin of Geological Society of America*, Vol. 86, 1975, pp. 1287-1295.
2. Burke, K., and Dewey, J. F., "Plume-Generated Triple Junctions - Key Indicators in Applying Plate Tectonics to Old Rocks," *Journal of Geology*, Vol. 81, 1973, pp. 406-433.
3. Braile, L. W., Hinze, W. J., Keller, G. R., and Lidiak, E. G., "The Northern Extension of the New Madrid Fault Seismic Zone," *in* McKeown, F. A., and Pakiser, L. C., eds., *Investigations of the New Madrid, Missouri, Earthquake Region: U.S. Geological Survey Professional Paper 1236-L*, 1982, pp. 175-184.
4. Braile, L. W., Hinze, W. J., Sexton, J. L., Keller, G. R., and Lidiak, E. G., "Tectonic Development of the New Madrid Seismic Zone," *in* Gori, P. L., and Hays, W. W., eds., *Proceedings, Symposium on the New Madrid earthquakes: U.S. Geological Survey Open File Report 84-770*, 1984, pp. 204-233.
5. McKeown, F. A., "Overview and Discussion," *in* McKeown, F. A., and Pakiser, L. C., eds., *Investigations of the New Madrid, Missouri, Earthquake Region: U.S. Geological Survey Professional Paper 1236-A*, 1982, pp. 1-14.
6. O'Connell, D. R., Bufe, C. G., and Zoback, M. D., "Microearthquakes and Faulting in the Area of New Madrid, Missouri-Reelfoot Lake, Tennessee," *in* McKeown, F. A., and Pakiser, L. C., eds., *Investigations of the New Madrid, Missouri, Earthquake Region: U.S. Geological Survey Professional Paper 1236-D*, 1982, pp. 31-38.
7. Hildenbrand, T. G., "Rift Structure of the Northern Mississippi Embayment from the Analysis of Gravity and Magnetic Data," *Journal of Geophysical Research*, Vol. 90, No. B14, December, 1985, pp. 12,607-12,622.
8. Hildenbrand, T. G., Kane, M. F., and Hendricks, J. D., "Magnetic Basement in the Upper Mississippi Embayment Region - A Preliminary Report," *in* McKeown, F. A., and Pakiser, L. C., eds., *Investigations of the New Madrid, Missouri, Earthquake Region: U.S. Geological Survey Professional Paper 1236-E*, 1982, pp. 39-53.

9. Kane, M. F., Hildenbrand, T. G., and Hendricks, J. D., "A Model for the Tectonic Evolution of the Mississippi Embayment and its Contemporary Seismicity," *Geology*, Vol. 9, 1981, pp. 563-567.
10. Mooney, W. D., and Andrews, M. C., "Seismic Refraction Studies of the Mississippi Embayment," in Gori, P. L., and Hays, W. W., eds., *Proceedings, Symposium on the New Madrid Seismic Zone: U.S. Geological Survey Open File Report 84-770*, 1984, pp. 138-167.
11. Mooney, W. D., and Andrews, M. C., Ginzburg, D. A., Peters, D. A., and Hamilton, R. M., "Crustal Structure of the Mississippi Embayment and a Comparison with Other Continental Rift Zones: *Tectonophysics*, Vol. 94, 1983, pp. 327-348.
12. Herrmann, R. B., "Surface Wave Focal Mechanisms for Eastern North American Earthquakes with Tectonic Implications: *Journal of Geophysical Research*," *Journal of Geophysical Research*, Vol. 84, No. 37, 1979, pp. 3543-3552.
13. Johnston, A. C., "A Major Earthquake Zone on the Mississippi," *Scientific American*, Vol. 246, No. 4, 1982, pp. 60-68.
14. Stauder, W., "Present-Day Seismicity and Identification of Active Faults in the New Madrid Seismic Zone," in McKeown, F. A., and Pakiser, L. C., eds., *Investigations of the New Madrid, Missouri, Earthquake Region: U.S. Geological Survey Professional Paper 1236-C*, 1982, pp. 1-14.
15. Herrmann, R. B., and Canas, J., "Focal Mechanism Studies in the New Madrid Seismic Zone," *Bulletin of the Seismological Society of America*, Vol. 68, No. 4, August, 1978, pp. 1095-1102.
16. Johnston, A. C., "Seismic Ground Motions in Shelby County, Tennessee, Resulting from Large New Madrid Earthquakes," *Technical Report of Center for Earthquake Research and Information, Memphis State University*, January, 1988.
17. Nuttli, O. W., "Seismic Wave Attenuation and Magnitude Relations for Eastern North America," *Journal of Geophysical Research*, Vol. 78, 1973, pp. 876-885.
18. Nuttli, O. W., "The Mississippi Valley Earthquakes of 1811 and 1812: Intensities, Ground Motion and Magnitudes," *Bulletin of the Seismological Society of America*, Vol. 63, No. 1, April, 1973, pp. 227-248.



19. Dwyer, J. J., Herrmann, R. B., and Nuttli, O. W., "Spatial Attenuation of the  $L_g$  Wave in the Central United States," Bulletin of the Seismological Society of America, Vol. 73, No. 3, June, 1983, pp. 781-796.
20. Hasegawa, H. S., "Attenuation of  $L_g$  Waves in the Canadian Shield," Bulletin of the Seismological Society of America, Vol. 75, No. 3, 1985, pp. 1569-1582.
21. Shin, T.-C., and Herrmann, R. B., " $L_g$  Attenuation and Source Studies Using 1982 Miramichi Data," Bulletin of the Seismological Society of America, Vol. 77, No. 2, April, 1987, pp. 384-397.
22. Joyner, W. B., and Boore, D. M., "Peak Horizontal Acceleration and Velocity from Strong-Motion Records Including Records from the 1981 Imperial Valley, California, Earthquake," Bulletin of the Seismological Society of America, Vol. 71, No. 6, December, 1981, pp. 2011-2038.
23. Joyner, W. B., and Boore, D. M., "Prediction of Earthquake Response Spectra," Proceedings, 51st Annual Convention Structural Engineering Association of California, also United States Geological Survey Open-File Report 82-799, 1982, 16 pp.
24. Nuttli, O. W. and Herrmann, R. B., "Ground Motion of Mississippi Valley Earthquakes," Journal of Technical Topics Civil Engineering, Vol. 110, No. 1, 1984, pp. 54-69.
25. Nuttli, O. W. and Herrmann, R. B., "Ground Motion Relations for Eastern North American Earthquake," Proceedings: 3rd International Conference on Soil Dynamics and Earthquake Engineering, Princeton, NJ. Vol. II, 1987, pp. 231-241.
26. Algermissen, S. T., and Perkins, D. M., "A Probabilistic Estimate of Maximum Acceleration in Rock in the Contiguous United States," United State Geological Survey Open-File Report 76-416, 1976, 45 pp.
27. Algermissen, S. T., and Perkins, D. M., Thenhaus, S. L., and Bender, B. L., "Probabilistic Estimate of Maximum Acceleration and Velocity in Rock in the Contiguous United States," United State Geological Survey Open-File Report 82-1033, 1982, 99 pp.
28. Boore, D. M., "Stochastic Simulation of High-Frequency Ground Motions Based on Seismological Models of the Radiated Spectra," Bulletin of the Seismological Society of America, Vol. 73, No. 6, December, 1983, pp. 1864-1894.

29. Boore, D. M., and Atkinson, G. M., "Stochastic Prediction of Ground Motion and Spectral Response Parameters at Hard-Rock Sites in Eastern North America," *Bulletin of the Seismological Society of America*, Vol. 77, No. 2, April, 1987, pp. 440-467.
30. Joyner, W. B., and Boore, D. M., "Measurement, Characterization, and Prediction of Strong Ground Motion," *Proceedings, Earthquake Engineering and Soil Dynamics II GT Div/ASCE, Park City, Utah, June 27-30, 1988*,
31. McGuire, R. K., Toro, G. R., and Silva, W. J., "Engineering Model of Earthquake Ground Motion for Eastern North America," *Risk Engineering, INC., EPRI NP-6074*, October, 1988.
32. Papageorgiou, A. S., and Aki, K., "A Specific Barrier Model for the Quantitative Description of Inhomogeneous Faulting and the Prediction of Strong Ground Motion. I. Description of the Model," *Bulletin of the Seismological Society of America*, Vol. 73, 1983, pp. 693-722.
33. Toro, G. R., and McGuire, R. K., "An Investigation into Earthquake Ground Motion Characteristics in Eastern North America," *Bulletin of the Seismological Society of America*, Vol. 77, 1987, pp. 468-489.
34. Brune, J. N., "Tectonic Stress and Spectra of Seismic Shear Waves from Earthquakes," *Journal of Geophysical Research*, Vol. 75, No. 26, September, 1970, pp. 4997-5009.
35. Brune, J. N., "Correction," *Journal of Geophysical Research*, Vol. 76, No. 20, July, 1971, 5002.
36. Aki, K., "Scaling Law of Seismic Spectrum," *Journal of Geophysical Research*, Vol. 72, 1967, pp. 1217-1231.
37. Aki, K., "Generation of Propagation of G Waves from the Niigata Earthquake of June 16, 1964. 2. Estimation of Earthquake Movement, Released Energy, and stress-Strain Drop from G-Wave Spectrum," *Bulletin of Earthquake Research Institute, Tokyo University*. Vol. 44, 1966, pp. 23-88.
38. Hanks, T. C., and Kanamori, H., "A Moment Magnitude Scale," *Journal of Geophysical Research*, Vol. 84, No. B5, 1979, pp. 2348-2350.

39. Joyner, W. B., "A Scaling Law for the Spectra of Large Earthquakes," *Bulletin of the Seismological Society of America*, Vol. 74, No. 4, August, 1984, pp. 1167-1188.
40. Atkinson, G. M., "Ground Motions of Moderate Earthquakes Recorded by the Eastern Canada Telemetered Network," Geological Survey of Canada, Earth Physics Branch Open-File No. 85-5, Ottawa, 1985, 76 pp.
41. Nuttli, O. W., "Average Seismic Source-Parameter Relations for Mid-Plate Earthquakes," *Bulletin of the Seismological Society of America*, Vol. 73, No. 2, April, 1983, pp. 519-535.
42. Somerville, P. G., McLaren, J. P., LeFevre, L. V., Burger, R. W., and Helmberger, D. V., "Comparison of Source Scaling Relations of Eastern and Western North American Earthquakes," *Bulletin of the Seismological Society of America*, Vol. 77, 1987, pp. 322-346.
43. Mcguire, R. K., Becker, A. M., Donovan, N. C., "Spectral Estimates of Seismic Shear Waves," *Bulletin of the Seismological Society of America*, Vol. 74, 1984, pp. 1427-1440.
44. Nebelek, J. and Saurez, G., "The 1983 Goodnow Earthquake in the Central Adirondacks, NY: A Broadband Teleseismic Analysis," Technical Report NCEER-87-0025, Center for Earthquake Engineering Research, SUNY, Buffalo, NY, 1987, pp. 300-317.
45. Boore, D. M. and Boatwright J., "Average Body-Wave Radiation Coefficients," *Bulletin of the Seismological Society of America*, Vol. 74, No. 5, October, 1984, pp. 1615-1621.
46. Herrmann, R. B., and Kijko, A., "Modeling Some Empirical Vertical Component  $L_g$  Relations," *Bulletin of the Seismological Society of America*, Vol. 73, No. 1, February, 1983, pp. 157-171.
47. Moayyad, P. and Mohraz, B., "A Study of Power Spectral Density of Earthquake Accelerograms," Civil and Mechanical Engineering Department, Southern Methodist University, Dallas, Texas, June, 1982.
48. Hanks, T. C., " $b$ -values and  $\omega^{-\gamma}$  Seismic Source Models: Implications for Tectonic Stress Variations Along Active Crustal Fault Zones and the Estimation of High-Frequency Strong Ground Motion," *Journal of Geophysical Research*, Vol. 84, 1979, pp. 2235-2242.

49. McGuire, R. K., and Hanks, T. C., "RMS Accelerations and Spectral Amplitudes of Strong Ground Motion During the San Fernando, California Earthquake," *Bulletin of the Seismological Society of America*, Vol. 70, No. 5, October, 1980, pp. 1907-1919.
50. Shinozuka, M., "Digital Simulation of Ground Acceleration," *Proceedings of the 5th World Conference on Earthquake Engineering*, Rome, Italy, June, 1973, pp. 2829-2838.
51. Shinozuka, M., "Digital Simulation of Random Processes in Engineering Mechanics with the aid of FFT Technique," *in Ariaratnam, S. T., and Leipholz, H. H. E., eds., Stochastic Problems in Mechanics*, University of Waterloo Press, Waterloo, 1974, pp. 277-286.
52. Hwang, H., Pires, J., and Chokshi N. C., "Generation of Consistent Power/Response Spectra," *Proceedings of the 8th SMiRT conference*, Vol. K, Paper K1 12/3, August 19-23, 1985.
53. Johnston, A. C., and Nava, S. J., "Recurrence Rates and Probability Estimates for the New Madrid Seismic Zone," *Journal of Geophysical Research*, Vol. 90, No. B8, July, 1985, pp. 6737-6753.
54. Ng, K. W., Chang, T.-S., and Hwang, H., "Subsurface Conditions of Memphis and Shelby County," *Technical Report NCEER-89-0021*, National Center for Earthquake Engineering Research, SUNY, Buffalo, NY, July, 1989.
55. Nuttli, O. W., "Damaging Earthquakes of the Central Mississippi Valley," *in McKown F. A., and Pakiser, L. C., eds., Investigations of the New Madrid, Missouri, Earthquake Region: U.S. Geological Survey Professional Paper 1236-B*, 1982, pp. 15-20.
56. Hwang, H., Low, Y. K. and Chang, T.-S. "Seismic Response Study of Two Memphis Sites," *in Kauhawy, F. H., ed., Foundation Engineering: Current Principles and Practices*, Vol. 1, ASCE, 1989, pp. 786-798.

## APPENDIX A

### EXTREME VALUE DISTRIBUTION OF A RANDOM PROCESS

Assuming that  $y(t)$  is a stationary Gaussian process with mean zero and one-sided power spectrum  $S_y(\omega)$ . The variance of the process  $\sigma_y^2$  is

$$\sigma_y^2 = \int_0^{\infty} S_y(\omega) d\omega \quad (A.1)$$

and the moments of the spectral density function about the frequency origin are

$$\lambda_i = \int_0^{\infty} \omega^i S_y(\omega) d\omega, \quad i = 0, 1, 2, \dots \quad (A.2)$$

It is noted that  $\lambda_0$  is equal to  $\sigma_y^2$  and the second moment  $\lambda_2$  is the variance of its time derivative  $\sigma_{\dot{y}}^2$ . The shape factor  $\delta$  is defined as

$$\delta = \sqrt{1 - \lambda_1^2 / (\lambda_0 \lambda_2)} \quad (A.3)$$

The shape factor is a measure of the dispersion of the spectral density function about its center frequency.  $\delta$  is dimensionless and always lies between 0 and 1. Furthermore,  $\delta$  is small for a narrow-band process and relatively large for a wide-band process [A.1].

The mean zero-crossing rate of the stationary Gaussian process  $\nu_0$  is

$$\nu_0 = \frac{1}{\pi} \frac{\sigma_{\dot{y}}}{\sigma_y} = \frac{1}{\pi} \sqrt{\lambda_2 / \lambda_0} \quad (A.4)$$

The maximum absolute value of a stationary random process  $y(t)$  over a duration  $T_d$  is defined as:

$$y_m = \max|y(t)|, \quad 0 \leq t \leq T_d \quad (A.5)$$

The statistical distribution of  $y_m$  can be approximated by the asymptotic distribution function of the extreme values [A.2]. In this study, however, the cumulative distribution function of  $y_m$  proposed by Vanmarcke [A.1] is used,

$$F_{y_m}(r) = \left[1 - \exp\left(-\frac{a^2}{2}\right)\right] \exp\left[-\nu_0 T_d \frac{1 - \exp\left(-\sqrt{\pi/2} a \delta_e\right)}{\exp(a^2/2) - 1}\right]; \quad r > 0 \quad (A.6)$$

in which  $\delta_e = \delta^{1.2}$  and  $a = \tau/\sqrt{\lambda_0}$  is a normalized barrier level.

The mean and standard deviation of  $y_m$  are particularly useful to engineering applications. The mean value  $\bar{y}_m$  and standard deviation  $\sigma_{y_m}$  can be expressed as follows:

$$\bar{y}_m = p_m \cdot \sigma_y \quad (A.7)$$

$$\sigma_{y_m} = q \cdot \sigma_y \quad (A.8)$$

From equation (A.6), Der Kiureghian [A.3] obtained the following empirical equations for  $p_m$  and  $q$ :

$$p_m = \sqrt{2 \ln(\nu_e T_d)} + 0.5772 / \sqrt{2 \ln(\nu_e T_d)} \quad (A.9)$$

$$q = 1.2 / \sqrt{2 \ln(\nu_e T_d)} - 5.4 / (13 + [2 \ln(\nu_e T_d)]^{3.2}) \quad (A.10)$$

in which

$$\nu_e T_d = \begin{cases} \max(2.1, 2\delta\nu_0 T_d); & 0.00 < \delta \leq 0.10 \\ (1.63\delta^{0.45} - 0.38)\nu_0 T_d; & 0.10 < \delta < 0.69 \\ \nu_0 T_d & 0.69 \leq \delta < 1.00 \end{cases} \quad (A.11)$$

## References

- A.1 Vanmarcke, E. H., "On the Distribution of First Passage Times for Normal Stationary Random Processes," *Journal of Applied Mechanics*, ASME, Vol. 42, March, 1975, pp. 215-220.
- A.2 Shinozuka, M., "Methods of Safety and Reliability Analysis," *in* Freudenthal, A. M., ed., *Proceedings, International Conference on Structural Safety and Reliability*, Washington, D. C., April, 9-11, 1969, pp. 11-45.
- A.3 Der Kiureghian, A., Sackman, J. L., and Nour-Omid, B., "Dynamic Analysis of Light Equipment in Structures: Response to Stochastic Input," *Journal of Engineering Mechanics Division*, ASCE, Vol. 109, No. EM1, February, 1983, pp. 90-110.

**NATIONAL CENTER FOR EARTHQUAKE ENGINEERING RESEARCH  
LIST OF PUBLISHED TECHNICAL REPORTS**

The National Center for Earthquake Engineering Research (NCEER) publishes technical reports on a variety of subjects related to earthquake engineering written by authors funded through NCEER. These reports are available from both NCEER's Publications Department and the National Technical Information Service (NTIS). Requests for reports should be directed to the Publications Department, National Center for Earthquake Engineering Research, State University of New York at Buffalo, Red Jacket Quadrangle, Buffalo, New York 14261. Reports can also be requested through NTIS, 5285 Port Royal Road, Springfield, Virginia 22161. NTIS accession numbers are shown in parenthesis, if available.

- NCEER-87-0001 "First-Year Program in Research, Education and Technology Transfer," 3/5/87, (PB88-134275/AS).
- NCEER-87-0002 "Experimental Evaluation of Instantaneous Optimal Algorithms for Structural Control," by R.C. Lin, T.T. Soong and A.M. Reinhorn, 4/20/87, (PB88-134341/AS).
- NCEER-87-0003 "Experimentation Using the Earthquake Simulation Facilities at University at Buffalo," by A.M. Reinhorn and R.L. Ketter, to be published.
- NCEER-87-0004 "The System Characteristics and Performance of a Shaking Table," by J.S. Hwang, K.C. Chang and G.C. Lee, 6/1/87, (PB88-134259/AS).
- NCEER-87-0005 "A Finite Element Formulation for Nonlinear Viscoplastic Material Using a Q Model," by O. Gyebe and G. Dasgupta, 11/2/87, (PB88-213764/AS).
- NCEER-87-0006 "Symbolic Manipulation Program (SMP) - Algebraic Codes for Two and Three Dimensional Finite Element Formulations," by X. Lee and G. Dasgupta, 11/9/87, (PB88-219522/AS).
- NCEER-87-0007 "Instantaneous Optimal Control Laws for Tall Buildings Under Seismic Excitations," by J.N. Yang, A. Akbarpour and P. Ghaemmaghami, 6/10/87, (PB88-134333/AS).
- NCEER-87-0008 "IDARC: Inelastic Damage Analysis of Reinforced Concrete Frame - Shear-Wall Structures," by Y.J. Park, A.M. Reinhorn and S.K. Kunmath, 7/20/87, (PB88-134325/AS).
- NCEER-87-0009 "Liquefaction Potential for New York State: A Preliminary Report on Sites in Manhattan and Buffalo," by M. Budhu, V. Vijayakumar, R.F. Giese and L. Baumgras, 8/31/87, (PB88-163704/AS). This report is available only through NTIS (see address given above).
- NCEER-87-0010 "Vertical and Torsional Vibration of Foundations in Inhomogeneous Media," by A.S. Veletsos and K.W. Dotson, 6/1/87, (PB88-134291/AS).
- NCEER-87-0011 "Seismic Probabilistic Risk Assessment and Seismic Margins Studies for Nuclear Power Plants," by Howard H.M. Hwang, 6/15/87, (PB88-134267/AS). This report is available only through NTIS (see address given above).
- NCEER-87-0012 "Parametric Studies of Frequency Response of Secondary Systems Under Ground-Acceleration Excitations," by Y. Yong and Y.K. Lin, 6/10/87, (PB88-134309/AS).
- NCEER-87-0013 "Frequency Response of Secondary Systems Under Seismic Excitation," by J.A. HoLung, J. Cai and Y.K. Lin, 7/31/87, (PB88-134317/AS).
- NCEER-87-0014 "Modelling Earthquake Ground Motions in Seismically Active Regions Using Parametric Time Series Methods," by G.W. Ellis and A.S. Cakmak, 8/25/87, (PB88-134283/AS).
- NCEER-87-0015 "Detection and Assessment of Seismic Structural Damage," by E. DiPasquale and A.S. Cakmak, 8/25/87, (PB88-163712/AS).
- NCEER-87-0016 "Pipeline Experiment at Parkfield, California," by J. Isenberg and E. Richardson, 9/15/87, (PB88-163720/AS).

- NCEER-87-0017 "Digital Simulation of Seismic Ground Motion," by M. Shinozuka, G. Deodatis and T. Harada, 8/31/87, (PB88-155197/AS). This report is available only through NTIS (see address given above).
- NCEER-87-0018 "Practical Considerations for Structural Control: System Uncertainty, System Time Delay and Truncation of Small Control Forces," J.N. Yang and A. Akbarpour, 8/10/87, (PB88-163738/AS).
- NCEER-87-0019 "Modal Analysis of Nonclassically Damped Structural Systems Using Canonical Transformation," by J.N. Yang, S. Sarkani and F.X. Long, 9/27/87, (PB88-187851/AS).
- NCEER-87-0020 "A Nonstationary Solution in Random Vibration Theory," by J.R. Red-Horse and P.D. Spanos, 11/3/87, (PB88-163746/AS).
- NCEER-87-0021 "Horizontal Impedances for Radially Inhomogeneous Viscoelastic Soil Layers," by A.S. Veletsos and K.W. Dotson, 10/15/87, (PB88-150859/AS).
- NCEER-87-0022 "Seismic Damage Assessment of Reinforced Concrete Members," by Y.S. Chung, C. Meyer and M. Shinozuka, 10/9/87, (PB88-150867/AS). This report is available only through NTIS (see address given above).
- NCEER-87-0023 "Active Structural Control in Civil Engineering," by T.T. Soong, 11/11/87, (PB88-187778/AS).
- NCEER-87-0024 "Vertical and Torsional Impedances for Radially Inhomogeneous Viscoelastic Soil Layers," by K.W. Dotson and A.S. Veletsos, 12/87, (PB88-187786/AS).
- NCEER-87-0025 "Proceedings from the Symposium on Seismic Hazards, Ground Motions, Soil-Liquefaction and Engineering Practice in Eastern North America," October 20-22, 1987, edited by K.H. Jacob, 12/87, (PB88-188115/AS).
- NCEER-87-0026 "Report on the Whittier-Narrows, California, Earthquake of October 1, 1987," by J. Pantelic and A. Reinhorn, 11/87, (PB88-187752/AS). This report is available only through NTIS (see address given above).
- NCEER-87-0027 "Design of a Modular Program for Transient Nonlinear Analysis of Large 3-D Building Structures," by S. Srivastav and J.F. Abel, 12/30/87, (PB88-187950/AS).
- NCEER-87-0028 "Second-Year Program in Research, Education and Technology Transfer," 3/8/88, (PB88-219480/AS).
- NCEER-88-0001 "Workshop on Seismic Computer Analysis and Design of Buildings With Interactive Graphics," by W. McGuire, J.F. Abel and C.H. Conley, 1/18/88, (PB88-187760/AS).
- NCEER-88-0002 "Optimal Control of Nonlinear Flexible Structures," by J.N. Yang, F.X. Long and D. Wong, 1/22/88, (PB88-213772/AS).
- NCEER-88-0003 "Substructuring Techniques in the Time Domain for Primary-Secondary Structural Systems," by G.D. Manolis and G. Juhn, 2/10/88, (PB88-213780/AS).
- NCEER-88-0004 "Iterative Seismic Analysis of Primary-Secondary Systems," by A. Singhal, L.D. Lutes and P.D. Spanos, 2/23/88, (PB88-213798/AS).
- NCEER-88-0005 "Stochastic Finite Element Expansion for Random Media," by P.D. Spanos and R. Ghanem, 3/14/88, (PB88-213806/AS).
- NCEER-88-0006 "Combining Structural Optimization and Structural Control," by F.Y. Cheng and C.P. Pantelides, 1/10/88, (PB88-213814/AS).
- NCEER-88-0007 "Seismic Performance Assessment of Code-Designed Structures," by H.H-M. Hwang, J-W. Jaw and H-J. Shau, 3/20/88, (PB88-219423/AS).



- NCEER-88-0008 "Reliability Analysis of Code-Designed Structures Under Natural Hazards," by H.H-M. Hwang, H. Ushiba and M. Shinozuka, 2/29/88, (PB88-229471/AS).
- NCEER-88-0009 "Seismic Fragility Analysis of Shear Wall Structures," by J-W Jaw and H.H-M. Hwang, 4/30/88, (PB89-102867/AS).
- NCEER-88-0010 "Base Isolation of a Multi-Story Building Under a Harmonic Ground Motion - A Comparison of Performances of Various Systems," by F-G Fan, G. Ahmadi and I.G. Tadjbakhsh, 5/18/88, (PB89-122238/AS).
- NCEER-88-0011 "Seismic Floor Response Spectra for a Combined System by Green's Functions," by F.M. Lavelle, L.A. Bergman and P.D. Spanos, 5/1/88, (PB89-102875/AS).
- NCEER-88-0012 "A New Solution Technique for Randomly Excited Hysteretic Structures," by G.Q. Cai and Y.K. Lin, 5/16/88, (PB89-102883/AS).
- NCEER-88-0013 "A Study of Radiation Damping and Soil-Structure Interaction Effects in the Centrifuge," by K. Weissman, supervised by J.H. Prevost, 5/24/88, (PB89-144703/AS).
- NCEER-88-0014 "Parameter Identification and Implementation of a Kinematic Plasticity Model for Frictional Soils," by J.H. Prevost and D.V. Griffiths, to be published.
- NCEER-88-0015 "Two- and Three- Dimensional Dynamic Finite Element Analyses of the Long Valley Dam," by D.V. Griffiths and J.H. Prevost, 6/17/88, (PB89-144711/AS).
- NCEER-88-0016 "Damage Assessment of Reinforced Concrete Structures in Eastern United States," by A.M. Reinhorn, M.J. Seidel, S.K. Kunnath and Y.J. Park, 6/15/88, (PB89-122220/AS).
- NCEER-88-0017 "Dynamic Compliance of Vertically Loaded Strip Foundations in Multilayered Viscoelastic Soils," by S. Ahmad and A.S.M. Israil, 6/17/88, (PB89-102891/AS).
- NCEER-88-0018 "An Experimental Study of Seismic Structural Response With Added Viscoelastic Dampers," by R.C. Lin, Z. Liang, T.T. Soong and R.H. Zhang, 6/30/88, (PB89-122212/AS).
- NCEER-88-0019 "Experimental Investigation of Primary - Secondary System Interaction," by G.D. Manolis, G. Juhn and A.M. Reinhorn, 5/27/88, (PB89-122204/AS).
- NCEER-88-0020 "A Response Spectrum Approach For Analysis of Nonclassically Damped Structures," by J.N. Yang, S. Sarkani and F.X. Long, 4/22/88, (PB89-102909/AS).
- NCEER-88-0021 "Seismic Interaction of Structures and Soils: Stochastic Approach," by A.S. Veletsos and A.M. Prasad, 7/21/88, (PB89-122196/AS).
- NCEER-88-0022 "Identification of the Serviceability Limit State and Detection of Seismic Structural Damage," by E. DiPasquale and A.S. Cakmak, 6/15/88, (PB89-122188/AS).
- NCEER-88-0023 "Multi-Hazard Risk Analysis: Case of a Simple Offshore Structure," by B.K. Bhartia and E.H. Vanmarcke, 7/21/88, (PB89-145213/AS).
- NCEER-88-0024 "Automated Seismic Design of Reinforced Concrete Buildings," by Y.S. Chung, C. Meyer and M. Shinozuka, 7/5/88, (PB89-122170/AS).
- NCEER-88-0025 "Experimental Study of Active Control of MDOF Structures Under Seismic Excitations," by L.L. Chung, R.C. Lin, T.T. Soong and A.M. Reinhorn, 7/10/88, (PB89-122600/AS).
- NCEER-88-0026 "Earthquake Simulation Tests of a Low-Rise Metal Structure," by J.S. Hwang, K.C. Chang, G.C. Lee and R.L. Ketter, 8/1/88, (PB89-102917/AS).
- NCEER-88-0027 "Systems Study of Urban Response and Reconstruction Due to Catastrophic Earthquakes," by F. Kozin and H.K. Zhou, 9/22/88.

- NCEER-88-0028 "Seismic Fragility Analysis of Plane Frame Structures," by H.H-M. Hwang and Y.K. Low, 7/31/88, (PB89-131445/AS).
- NCEER-88-0029 "Response Analysis of Stochastic Structures," by A. Kardara, C. Bucher and M. Shinozuka, 9/22/88, (PB89-174429/AS).
- NCEER-88-0030 "Nonnormal Accelerations Due to Yielding in a Primary Structure," by D.C.K. Chen and L.D. Lutes, 9/19/88, (PB89-131437/AS).
- NCEER-88-0031 "Design Approaches for Soil-Structure Interaction," by A.S. Veletsos, A.M. Prasad and Y. Tang, 12/30/88, (PB89-174437/AS).
- NCEER-88-0032 "A Re-evaluation of Design Spectra for Seismic Damage Control," by C.J. Turkstra and A.G. Tallin, 11/7/88, (PB89-145221/AS).
- NCEER-88-0033 "The Behavior and Design of Noncontact Lap Splices Subjected to Repeated Inelastic Tensile Loading," by V.E. Sagan, P. Gergely and R.N. White, 12/8/88, (PB89-163737/AS).
- NCEER-88-0034 "Seismic Response of Pile Foundations," by S.M. Mamoon, P.K. Banerjee and S. Ahmad, 11/1/88, (PB89-145239/AS).
- NCEER-88-0035 "Modeling of R/C Building Structures With Flexible Floor Diaphragms (IDARC2)," by A.M. Reinhorn, S.K. Kunnath and N. Panahshahi, 9/7/88, (PB89-207153/AS).
- NCEER-88-0036 "Solution of the Dam-Reservoir Interaction Problem Using a Combination of FEM, BEM with Particular Integrals, Modal Analysis, and Substructuring," by C-S. Tsai, G.C. Lee and R.L. Ketter, 12/31/88, (PB89-207146/AS).
- NCEER-88-0037 "Optimal Placement of Actuators for Structural Control," by F.Y. Cheng and C.P. Pantelides, 8/15/88, (PB89-162846/AS).
- NCEER-88-0038 "Teflon Bearings in Aseismic Base Isolation: Experimental Studies and Mathematical Modeling," by A. Mokka, M.C. Constantinou and A.M. Reinhorn, 12/5/88, (PB89-218457/AS).
- NCEER-88-0039 "Seismic Behavior of Flat Slab High-Rise Buildings in the New York City Area," by P. Weidlinger and M. Ettouney, 10/15/88.
- NCEER-88-0040 "Evaluation of the Earthquake Resistance of Existing Buildings in New York City," by P. Weidlinger and M. Ettouney, 10/15/88, to be published.
- NCEER-88-0041 "Small-Scale Modeling Techniques for Reinforced Concrete Structures Subjected to Seismic Loads," by W. Kim, A. El-Attar and R.N. White, 11/22/88, (PB89-189625/AS).
- NCEER-88-0042 "Modeling Strong Ground Motion from Multiple Event Earthquakes," by G.W. Ellis and A.S. Cakmak, 10/15/88, (PB89-174445/AS).
- NCEER-88-0043 "Nonstationary Models of Seismic Ground Acceleration," by M. Grigoriu, S.E. Ruiz and E. Rosenblueth, 7/15/88, (PB89-189617/AS).
- NCEER-88-0044 "SARCF User's Guide: Seismic Analysis of Reinforced Concrete Frames," by Y.S. Chung, C. Meyer and M. Shinozuka, 11/9/88, (PB89-174452/AS).
- NCEER-88-0045 "First Expert Panel Meeting on Disaster Research and Planning," edited by J. Pantelic and J. Stoyke, 9/15/88, (PB89-174460/AS).
- NCEER-88-0046 "Preliminary Studies of the Effect of Degrading Infill Walls on the Nonlinear Seismic Response of Steel Frames," by C.Z. Chrysostomou, P. Gergely and J.F. Abel, 12/19/88, (PB89-208383/AS).

- NCEER-88-0047 "Reinforced Concrete Frame Component Testing Facility - Design, Construction, Instrumentation and Operation," by S.P. Pessiki, C. Conley, T. Bond, P. Gergely and R.N. White, 12/16/88, (PB89-174478/AS).
- NCEER-89-0001 "Effects of Protective Cushion and Soil Compliancy on the Response of Equipment Within a Seismically Excited Building," by J.A. HoLung, 2/16/89, (PB89-207179/AS).
- NCEER-89-0002 "Statistical Evaluation of Response Modification Factors for Reinforced Concrete Structures," by H.H-M. Hwang and J-W. Jaw, 2/17/89, (PB89-207187/AS).
- NCEER-89-0003 "Hysteretic Columns Under Random Excitation," by G-Q. Cai and Y.K. Lin, 1/9/89, (PB89-196513/AS).
- NCEER-89-0004 "Experimental Study of 'Elephant Foot Bulge' Instability of Thin-Walled Metal Tanks," by Z-H. Jia and R.L. Ketter, 2/22/89, (PB89-207195/AS).
- NCEER-89-0005 "Experiment on Performance of Buried Pipelines Across San Andreas Fault," by J. Isenberg, E. Richardson and T.D. O'Rourke, 3/10/89, (PB89-218440/AS).
- NCEER-89-0006 "A Knowledge-Based Approach to Structural Design of Earthquake-Resistant Buildings," by M. Subramani, P. Gergely, C.H. Conley, J.F. Abel and A.H. Zaghaw, 1/15/89, (PB89-218465/AS).
- NCEER-89-0007 "Liquefaction Hazards and Their Effects on Buried Pipelines," by T.D. O'Rourke and P.A. Lane, 2/1/89, (PB89-218481).
- NCEER-89-0008 "Fundamentals of System Identification in Structural Dynamics," by H. Imai, C-B. Yun, O. Maruyama and M. Shinozuka, 1/26/89, (PB89-207211/AS).
- NCEER-89-0009 "Effects of the 1985 Michoacan Earthquake on Water Systems and Other Buried Lifelines in Mexico," by A.G. Ayala and M.J. O'Rourke, 3/8/89, (PB89-207229/AS).
- NCEER-89-R010 "NCEER Bibliography of Earthquake Education Materials," by K.E.K. Ross, 3/10/89, (PB90-109901/AS).
- NCEER-89-0011 "Inelastic Three-Dimensional Response Analysis of Reinforced Concrete Building Structures (IDARC-3D), Part I - Modeling," by S.K. Kunnath and A.M. Reinhorn, 4/17/89.
- NCEER-89-0012 "Recommended Modifications to ATC-14," by C.D. Poland and J.O. Malley, 4/12/89.
- NCEER-89-0013 "Repair and Strengthening of Beam-to-Column Connections Subjected to Earthquake Loading," by M. Corazao and A.J. Durrani, 2/28/89, (PB90-109885/AS).
- NCEER-89-0014 "Program EXKAL2 for Identification of Structural Dynamic Systems," by O. Maruyama, C-B. Yun, M. Hoshiya and M. Shinozuka, 5/19/89, (PB90-109877/AS).
- NCEER-89-0015 "Response of Frames With Bolted Semi-Rigid Connections, Part I - Experimental Study and Analytical Predictions," by P.J. DiCorso, A.M. Reinhorn, J.R. Dickerson, J.B. Radzimirski and W.L. Harper, 6/1/89, to be published.
- NCEER-89-0016 "ARMA Monte Carlo Simulation in Probabilistic Structural Analysis," by P.D. Spanos and M.P. Mignolet, 7/10/89, (PB90-109893/AS).
- NCEER-89-0017 "Preliminary Proceedings of the Conference on Disaster Preparedness - The Place of Earthquake Education in Our Schools, July 9-11, 1989," 6/23/89, (PB90-108606/AS).
- NCEER-89-0018 "Multidimensional Models of Hysteretic Material Behavior for Vibration Analysis of Shape Memory Energy Absorbing Devices, by E.J. Graesser and F.A. Cozzarelli, 6/7/89.

- NCEER-89-0019 "Nonlinear Dynamic Analysis of Three-Dimensional Base Isolated Structures (3D-BASIS)," by S. Nagarajaiah, A.M. Reinhorn and M.C. Constantinou, 8/3/89.
- NCEER-89-0020 "Structural Control Considering Time-Rate of Control Forces and Control Rate Constraints," by F.Y. Cheng and C.P. Pantelides, 8/3/89.
- NCEER-89-0021 "Subsurface Conditions of Memphis and Shelby County," by K.W. Ng, T-S. Chang and H-H.M. Hwang, 7/26/89.
- NCEER-89-0022 "Seismic Wave Propagation Effects on Straight Jointed Buried Pipelines," by K. Elhadi and M.J. O'Rourke, 8/24/89.
- NCEER-89-0023 "Workshop on Serviceability Analysis of Water Delivery Systems," edited by M. Grigoriu, 3/6/89.
- NCEER-89-0024 "Shaking Table Study of a 1/5 Scale Steel Frame Composed of Tapered Members," by K.C. Chang, J.S. Hwang and G.C. Lee, 9/18/89.
- NCEER-89-0025 "DYNA1D: A Computer Program for Nonlinear Seismic Site Response Analysis - Technical Documentation," by Jean H. Prevost, 9/14/89.
- NCEER-89-0026 "1:4 Scale Model Studies of Active Tendon Systems and Active Mass Dampers for Aseismic Protection," by A.M. Reinhorn, T.T. Soong, R.C. Lin, Y.P. Yang, Y. Fukao, H. Abe and M. Nakai, 9/15/89, to be published.
- NCEER-89-0027 "Scattering of Waves by Inclusions in a Nonhomogeneous Elastic Half Space Solved by Boundary Element Methods," by P.K. Hadley, A. Askar and A.S. Cakmak, 6/15/89.
- NCEER-89-0028 "Statistical Evaluation of Deflection Amplification Factors for Reinforced Concrete Structures," by H.H.M. Hwang, J-W. Jaw and A.L. Ch'ng, 8/31/89.
- NCEER-89-0029 "Bedrock Accelerations in Memphis Area Due to Large New Madrid Earthquakes," by H.H.M. Hwang, C.H.S. Chen and G. Yu, 11/7/89.